

PART 3  
INVITED DISCOURSES

A. BY PROFESSOR J. A. VAN ALLEN

B. BY PROFESSOR M. SCHWARZSCHILD

C. BY ACADEMICIAN V. A. AMBARTSUMIAN

## INVITED DISCOURSE A

given to participants in the General Assembly at 16<sup>h</sup> 15<sup>m</sup> on Wednesday 16 August 1961 in the Auditorium of Wheeler Hall on the Berkeley Campus of the University of California by

**Professor James A. Van Allen**  
(*State University of Iowa, Iowa City, Iowa*)

on

### DYNAMICS, COMPOSITION AND ORIGIN OF THE GEOMAGNETICALLY-TRAPPED CORPUSCULAR RADIATION

#### INTRODUCTION

Before presenting his Invited Discourse, Professor Van Allen spoke as follows.

President Oort, Members of the International Astronomical Union, and Guests:

It is a great honor and privilege to participate in your meeting here in Berkeley and to speak on a topic which has a close kinship with solar, planetary and interplanetary astronomy, though it had its beginnings in a terrestrial setting.

Since sending the title of my paper to the General Secretary, I have decided to proceed in exactly the reverse manner to that indicated therein, and thus to discuss first the dynamics, second the composition, and third the origin of the corpuscular radiation, which is found to be temporarily trapped in the geomagnetic field. In this way, I proceed from the better understood to the less-well understood aspects of the subject.

#### 1.1 THE TRAPPING OF ELECTRICALLY CHARGED PARTICLES IN THE FIELD OF A MAGNETIC DIPOLE

In 1896, Birkeland (1908, 1913) undertook the experimental study of the motion of cathode rays under the influence of the magnetic field of a relatively isolated magnetic pole, and then of a magnetic dipole. The proper interpretation of the results obtained in the former case was given by Poincaré (1896) by integrating the equation of motion of a charged particle in the field of a magnetic unipole. The laboratory phenomena produced by Birkeland in the latter case were of a much more complex character. They were suggestive of the large-scale geophysical phenomena of the polar aurorae and inspired Störmer to undertake the detailed theoretical study of the motion of electrically charged particles in the field of a magnetic dipole. This undertaking occupied much of Störmer's professional career (Störmer, 1955).

The equation of motion of an isolated charged particle in a static magnetic field  $\mathbf{B}$  is:

$$\frac{d}{dt} \left( \frac{\mathbf{p}c}{Ze} \right) = \mathbf{v} \times \mathbf{B}, \quad (1.1)$$

wherein  $\mathbf{p}$  and  $\mathbf{v}$  are the vector momentum and velocity respectively of the particle,  $Ze$  is its electrical charge in e.s.u. and may be either positive or negative, and  $c$  is the speed of light. The scalar quantity  $pc/Ze$  is the magnetic rigidity  $R$  of the particle measured in units of electrical potential (ergs per unit charge if  $B$  is in gauss and c.g.s. units are used elsewhere; the

value of the magnetic rigidity in volts is found by multiplying its value in c.g.s. units by 300). The scalar magnitudes of  $\mathbf{p}$ ,  $R$  and  $\mathbf{v}$  are seen to be constants of the motion.

Thus, the differential equation of the spatial trajectory of the particle is

$$\left(\frac{R}{B}\right) \frac{d\mathbf{v}_1}{ds} = \mathbf{v}_1 \times \mathbf{B}_1. \tag{1.2}$$

In equation 1.2  $\mathbf{v}_1$  and  $\mathbf{B}_1$  are unit vectors parallel to  $\mathbf{v}$  and  $\mathbf{B}$  respectively and  $s$  is the arc length measured along the trajectory. All particles having the same magnetic rigidity  $R$  and a given  $\mathbf{v}_1$  at a specified point in a specified magnetic field have identical spatial trajectories. The time rate of traversal of the trajectory is proportional to  $v$ . The general relationship among magnetic rigidity, momentum, velocity and kinetic energy  $E$  is:

$$R \equiv \frac{pc}{Ze} = \frac{m_0c^2}{Ze} \frac{\beta}{(1 - \beta^2)^{1/2}} = \frac{(E^2 + 2Em_0c^2)^{1/2}}{Ze}, \tag{1.3}$$

$m_0$  being the rest mass,  $m_0c^2$  being the rest energy, and  $\beta$  being equal to  $v/c$ .

The field of a magnetic dipole  $M$ ,

$$\mathbf{B} = - \text{grad } \Omega = + \text{grad} \left( \frac{M \sin \lambda}{r^2} \right), \tag{1.4}$$

where  $\mathbf{M}$  is in the direction of the negative polar axis of a system of spherical coordinates,  $r, \lambda, \omega$ .

For the motion of a charged particle in such a field, Störmer obtained a first integral of equation (1.2) which may be written

$$\sin A = \frac{\cos \lambda}{(r/b)^2} + \frac{2(\gamma/b)}{(r/b) \cos \lambda}, \tag{1.5}$$

In (1.5)  $A$  is the angle between the velocity vector of the particle and its projection on the meridian plane through the particle,  $b \equiv (ZeM/pc)^{1/2}$  and  $\gamma$  is an arbitrary constant of integration.

Equation (1.5) may be rewritten as follows:

$$\frac{r}{b} = \frac{\cos^2 \lambda}{-(\gamma/b) \pm \{(\gamma/b)^2 + \sin A \cos^3 \lambda\}^{1/2}} \tag{1.6}$$

It is found that bounded motion is dynamically possible if and only if (neglecting special cases of little practical importance)

$$-\infty < (\gamma/b) < -1.$$

Subject to this condition there are two unconnected regions of possible motion (i.e.,  $r$  is positive real):

Region I:  $r_1 \leq r \leq r_2$  (Bounded Motion)

Region II:  $r \geq r_3$  (Unbounded Motion)

Region I, hereafter referred to as the "trapping region", is bounded by two surfaces of revolution about the axis of the magnetic dipole, viz.:

$$\frac{r_1}{b} = \frac{\cos^2 \lambda}{-(\gamma/b) + \{(\gamma/b)^2 + \cos^3 \lambda\}^{1/2}}, \tag{1.7a}$$

$$\frac{r_2}{b} = \frac{\cos^2 \lambda}{-(\gamma/b) + \{(\gamma/b)^2 - \cos^3 \lambda\}^{1/2}}, \tag{1.7b}$$

The inner boundary of Region II is the surface of revolution:

$$\frac{r_3}{b} = \frac{\cos^2 \lambda}{-(\gamma/b) - \{(\gamma/b)^2 - \cos^3 \lambda\}^{\frac{1}{2}}}, \tag{1.7c}$$

The detailed trajectory of a particle can be found only by numerical integration. None-the-less equations (1.7a, b, c) provide essential information of a general nature.

Störmer was primarily interested in trajectories from infinity and devoted only brief attention to those lying in Region I. He has published a numerically-calculated case of a bounded trajectory (Störmer, 1907) which will be utilized herein as an example of the general theory. The meridian projection of this trajectory is reproduced in Figure 1.1. It is, of course, understood that there is an accompanying motion in  $\omega$  which is not discussed here.

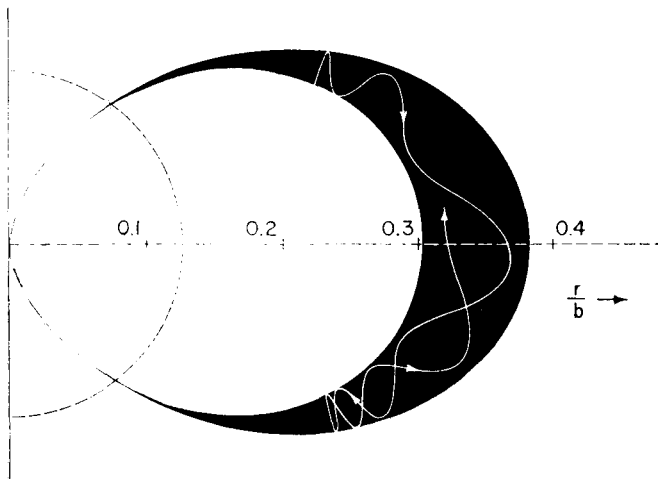


Fig. 1.1. A diagram after Störmer (1907), illustrating the meridian projection of the spatial trajectory of an electrically charged particle in the field of a magnetic dipole and the boundaries of the rigorous trapping region.

In present notation, the case of Figure 1.1 is characterized by the following, using the subscript zero to denote the values of parameters at injection:

$$\begin{aligned} (\gamma/b) &= -1.50 & \lambda_0 &= 26^\circ 29'.5 & \sin A_0 &= +1.0000 \\ (r_0/b) &= 0.24857 & \cos \lambda_0 &= 0.89500 \end{aligned}$$

Hence:

$$\begin{aligned} \frac{r_1}{b} &= \frac{\cos^2 \gamma}{1.50 + (2.25 + \cos^3 \lambda)^{\frac{1}{2}}} \\ \frac{r_2}{b} &= \frac{\cos^2 \lambda}{1.50 + (2.25 - \cos^3 \lambda)^{\frac{1}{2}}} \\ \frac{r_3}{b} &= \frac{\cos^2 \lambda}{1.50 - (2.25 - \cos^3 \lambda)^{\frac{1}{2}}} \end{aligned}$$

At  $\cos \lambda = 0.89500$ ,  $(r_1/b) = 0.24857$ ,  $(r_2/b) = 0.29254$  and  $(r_3/b) = 3.0597$ . Hence the injection conditions satisfy the condition  $r_1 \leq r \leq r_2$  and the particle is assuredly trapped forever thereafter. At the equator ( $\lambda = 0^\circ$ ),  $(r_1/b) = 0.30277$ ,  $(r_2/b) = 0.38197$  and  $(r_3/b) = 2.6180$ . (See Figure 1.1 wherein the linear scale of the diagram is given by  $(r/b) = 0.1$ , etc., on the horizontal axis).

A sample set of physical parameters corresponding to the above case of Störmer is the following:

$$\begin{aligned}
 pc &= 1.548 \times 10^{-3} \text{ erg (966 Mev)} \\
 Ze &= 4.80 \times 10^{-10} \text{ e.s.u.} \quad M = 8.06 \times 10^{25} \text{ gauss cm}^3 \\
 b &\equiv (ZeM/pc)^{1/2} = 5.0 \times 10^8 \text{ cm} \\
 r_0 &= 1.243 \times 10^9 \text{ cm} = 1.95 \text{ Earth radii} \\
 A_0 &= +90^\circ \quad \lambda_0 = 26^\circ 29'.5 \\
 r_1 \text{ (at } \lambda = 0^\circ) &= 1.514 \times 10^9 \text{ cm} = 2.38 \text{ Earth radii} \\
 r_2 \text{ (at } \lambda = 0^\circ) &= 1.910 \times 10^9 \text{ cm} = 3.00 \text{ Earth radii}
 \end{aligned}$$

The largest value of  $r_2$  always occurs at the equator  $\lambda = 0^\circ$  (for a given  $A$  and for  $(\gamma/b) < -1$ ). And when  $(\gamma/b) = -1$ ,  $r_2$  has a larger value than for any more negative value of  $(\gamma/b)$ . Hence the extreme outer radial limit of the trapping region is given by

$$r_{2 \text{ max}}/b = 1$$

The corresponding inner limit of  $r_1$  at  $\lambda = 0^\circ$  is

$$\frac{r_1}{b} = \frac{1}{1 + \sqrt{2}} \frac{r_{2 \text{ max}}}{b} = 0.414 \left( \frac{r_{2 \text{ max}}}{b} \right)$$

A convenient form of the first of the immediately preceding two equations as applied to the geomagnetic field is

$$(r_{2 \text{ max}})^2 = \frac{59.5 Z}{pc} \tag{1.8}$$

where  $r_{2 \text{ max}}$  in Earth radii (6371 km) is the extreme outer radial limit of the trapping region in the plane  $\lambda = 0^\circ$  for a particle of momentum  $p$  measured in units of  $10^9 \text{ ev}/c$  carrying  $Z$  electronic charges.

Table 1.1 gives a number of examples found by means of equation (1.8):

$r_{2 \text{ max}}$ Earth radii	Corresponding $r_1$ at $\lambda = 0$ Earth radii	$\frac{pc}{Z}$ Mev	$E$ proton Mev	$E$ electron Mev
1.00	0.41	$59.5 \times 10^3$	$58.6 \times 10^3$	$59.5 \times 10^3$
2.00	0.83	14.9	14.0	14.9
4.00	1.66	3.72	2.90	3.72
6.00	2.49	1.65	0.96	1.65
10.0	4.14	0.60	0.173	0.60
15.0	6.21	0.264	0.036	0.264

For the case of isolated non-interacting charged particles moving in the field of a static magnetic dipole in a vacuum, the Störmer theory of trapping has a certain measure of completeness. Given an adequate computational effort the motion of a particle can be found to any degree of detail desired.

Yet if one encloses the dipole by an impenetrable sphere centered on the dipole in an effort to apply the theory to the real geophysical case, one is immediately confronted by an essential question to which (to the author's knowledge) no satisfactory theoretical answer has been given. The question is:

'As a given trapped particle performs latitudinal and longitudinal excursions within the trapping region, is there a minimum radial distance of approach to the dipole  $r_{\min}$  which can be written in terms of the parameters of the problem?'

A rigorous answer to this question is of course desirable. Even if such does not exist, a quantitative, practical assessment of the matter would be very helpful.

The many published trajectories of Störmer and of others entitle one to the impression, and the hope, that it should be possible to provide an assessment of at least a statistical nature—in the form, for example, that a specified particle has a probability of 0.01 of approaching the dipole to a radial distance less than  $r_{\min}$  in  $10^7$  latitudinal excursions. There are four evident modes of attack on the matter:

(a) further study of the dynamical problem in the spirit of the work of Störmer and of Lemaître and Vallarta (Vallarta, 1938) on trajectories of particles coming from infinity, but with attention to the specific problem of trapped particles,

(b) a statistical mechanical study (Dresden, 1961),

(c) An extensive program of numerical computation using modern techniques,

(d) an experimental study.

The early magnetized terella experiments of Birkeland and the more recent ones of Bruche (1932), of Malmfors (1945), of Block (1955), and of Bennett (1959) have provided beautiful experimental exhibitions of trajectories leading from and leading to infinity and of apparently bounded trajectories. Yet due to gas scattering and other technical limitations no definitive quantitative answer to the central question at hand has been provided. Among recent experimental techniques in this field perhaps the one which holds the greatest promise is that of Gibson, Jordan and Lauer (1960). These workers have succeeded in confining positrons from the decay of  $\text{Ne}^{19}$  within a cylindrical 'magnetic mirror' machine in the laboratory for times of the order of 10 seconds; and since this trapping time was satisfactorily attributed to multiple scattering on the residual gas, it appears that the trapping time in a perfect vacuum must be at least an order of magnitude greater than 10 seconds and might be infinite. Relevant parameters of the experimental arrangement are as follows (derived and estimated from the published account):

Diameter of vacuum chamber:	50 cm
Length of vacuum chamber:	150 cm
Magnetic field in center of chamber:	1300 gauss
Magnetic field at ends:	2340 gauss
Typical Positron Energy:	1 Mev
Typical Positron Magnetic Rigidity:	4740 gauss cm
Diameter of Typical Larmor Circle:	~ 5 cm
Larmor frequency:	~ $2 \times 10^9 \text{ sec}^{-1}$
Mean trapped lifetime:	≥ 10 sec
Mean number of Larmor periods	> $2 \times 10^{10}$
Mean number of encounters with mirror:	> $10^8$ (approx.)
Value of $\rho \text{grad } B/B $ in vicinity of mirrors	~ 0.02

The quantitative implications of these results will be discussed in Section 1.2.

## 1.2 THE ALFVÉN APPROXIMATION

The tedium of the straightforward application of the Störmer trapping theory has been greatly reduced in many cases of practical importance by an approximate theory due to Alfvén. The Alfvén approximation provides a notably lucid and simple foundation for visualizing the motion of magnetically trapped particles and for discussing many detailed theoretical matters. Moreover it provides an answer, under certain conditions, to the question posed in the latter part of Section 1.1.

The basis of this theory is paraphrased from Alfvén (1950) as follows. In the case when the path of a charged particle makes many loops in the region of a magnetic field which is of interest, the linear dimensions of one loop are small compared to the dimensions of the region; and during a single turn (in many practical cases) the particle is moving in an approximately homogeneous field. The detailed plotting of the trajectory by numerical methods is often beyond practicality. Moreover such detail may be of little or no interest. Alfvén, therefore, proposes first to calculate the motion in a homogeneous field, then treat the inhomogeneity as a perturbation.

In an homogeneous field the motion of a charged particle is a helical one, composed of a uniform motion parallel to the field  $\mathbf{B}$  and a circular motion in a plane perpendicular to  $\mathbf{B}$ . The center of the instantaneous circle is called the guiding center of the particle's trajectory. Thus the motion of the particle in an homogeneous field may be represented as equivalent to the uniform linear motion of its guiding center parallel to  $\mathbf{B}$ . In the Alfvén approximation, the spiraling particle is regarded as an elementary magnetic dipole (Amperian current loop). The motion of the guiding center is then the motion of this dipole. The scalar value  $\mu$  of the dipole moment is the product of the area of the particle's loop projected perpendicular to  $\mathbf{B}$  multiplied by the equivalent current flowing in the loop, viz:

$$\mu = (\pi\rho^2) (Zev/c)$$

with  $\rho$  being the radius of the loop and  $\nu$  the Larmor frequency. By equation (1.1) the magnetic moment is found to be

$$\mu = \frac{p_{\perp}^2(1 - \beta^2)^{\frac{1}{2}}}{2 m B} \quad (1.9)$$

In (1.9),  $p_{\perp} = p \sin \alpha$ , the component of  $\mathbf{p}$  perpendicular to the magnetic field with  $\alpha$  the angle between  $\mathbf{p}$  and  $\mathbf{B}$ ;  $\beta = v/c$  is a constant of the motion; and  $m$  is the rest mass of the particle.

In a uniform, time-stationary magnetic field  $\mu$  is obviously a constant of the motion. Moreover, Alfvén has shown that even in a non-uniform, time-varying magnetic field  $\mu$  is an adiabatic invariant of the motion provided

$$\rho |\text{grad } B/B| \ll 1 \quad (1.10)$$

and

$$\frac{1}{B\nu} \left| \frac{\partial B}{\partial t} \right| \ll 1. \quad (1.11)$$

The precise nature of the conservation of  $\mu$  is important to its application to the discussion of geomagnetic trapping. This subject is under theoretical study, particularly by those engaged in the study of magnetic confinement in proposed controlled-thermonuclear devices. A crucial question is whether departures from constancy are of such a nature as to lead to loss of particles from a trapped condition within a finite time which may be specified in terms of the parameters of the physical situation. The question is similar to the one posed in the latter portion of Section 1.1. This may be seen as follows:

If indeed  $\mu$  is constant, then it follows from equation (1.9) that

$$\sin^2\alpha/B = \text{constant} \tag{1.12}$$

On a given line of force (along which the guiding center of a particle moves)  $B$  has its minimum value  $B_0$  in the equatorial plane ( $\lambda = 0^\circ$ ). Hence  $\alpha$  also has its minimum value  $\alpha_0$  there. The mirror point (or turning point) of the trajectory of the guiding center occurs at such a value of  $B$  that  $\alpha = \frac{1}{2}\pi$  or

$$B_M = B_0/\sin^2 \alpha_0 \tag{1.13}$$

Hence the motion of the guiding center is seen to be one of an oscillatory nature between two conjugate mirror points in opposite hemispheres, the scalar magnitude of  $B$  at the two being identical and given by equation (1.13), a result which is independent of the magnitude of the mass, charge or energy of the particle provided that conditions (1.10) and 1.11) are met. The guiding center of the particle also undergoes a monotonic, though non-uniform, drift in longitude which is discussed in a later section.

The rigorous theory of Störmer assures that a particle, once injected into a region in space defined in Section 1.1, will forever execute bounded motion (in the absence of physical perturbation). This condition, of course, continues to apply to the motion as discussed under the Alfvén approximation; that is to say, the motion of the particle is bounded between two known surfaces of revolution. Moreover if  $\mu$  is strictly conserved the two loci of conjugate mirror points are small circles formed by the intersection of cones, of half angle  $\frac{1}{2}\pi \pm \lambda_M$  and having axes parallel to the dipole, with the central curved surface of the Störmer trapping region. To the extent that  $\mu$  is *not* conserved, the following questions arise:

- (a) Does the mirror latitude  $\pm \lambda_M$  merely oscillate in a regular or in an irregular manner over a bounded finite range  $\lambda'_M$  to  $\lambda''_M$  about a mean value which is obtained from equation (1.13)? If so can the limits of the range  $\lambda'_M$  and  $\lambda''_M$  be specified in terms of the parameters of the physical problem?
- (b) Or does the mirror latitude move progressively or diffuse away from some initial value  $\lambda_{M0}$  such that after a sufficient number of latitudinal cycles it may have any value between  $\frac{1}{2}\pi$  and 0? If so, can there be found a function  $P(n, \lambda_M, \lambda_{M0})$  which gives the probability that a mirror latitude  $\lambda_M$  will have been reached after  $n$  cycles?

As mentioned earlier, the experiments of Gibson *et al* (1960) and the independent ones of Rodionov (1960) appear to provide the best available quantitative answers at present.

Further discussion of this matter is deferred to a later section. Meanwhile it is supposed that  $\mu$  is conserved.

### 1.3 CHARACTERISTIC TIMES IN GEOMAGNETIC TRAPPING

The dynamical motion of geomagnetically trapped particles may be regarded as the composite of three forms of cyclic motion. The first of these, characterized by the Larmor period  $\tau_1$ , is the circular motion of the particle around its guiding center. The second, with period  $\tau_2$ , is the cyclic motion of the guiding center between mirror points. The third is the longitudinal drift of the guiding center around the Earth with period  $\tau_3$ .

Visualization of the motion and of the foundations for discussing departures from a simple quiescent state depend in an essential way on a knowledge of the magnitudes of the respective cyclic periods:

$$\tau_1 = \frac{2\pi mc}{ZeB(1 - \beta^2)^{\frac{1}{2}}} \tag{1.14}$$

E\*

irrespective of the pitch angle  $\alpha$ . At radius  $r_0$  in the plane of the geomagnetic equator, for example,

$$\tau_1 = 1.146 \times 10^{-6} \frac{m r_0^3}{Z (1 - \beta^2)^{3/2}} \text{ seconds,} \tag{1.15}$$

where  $m$  is the rest mass of the particle measured in electron masses and  $r_0$  is measured in Earth radii. For the present purpose it is sufficient to note that the Larmor periods of trapped electrons are in the general range 1 to 1000 micro-seconds and of trapped protons in the general range 2 to 1000 milli-seconds.

$$\tau_2 = 4 \int_0^{\lambda_M} \frac{ds}{v_{\parallel}} \tag{1.16}$$

with  $ds$  the arc length along the line of force followed by the guiding center and  $v_{\parallel}$  the component of velocity of the particle parallel to  $\mathbf{B}$ . As a consequence of equation (1.12),

$$v_{\parallel} = v (1 - B/B_M)^{1/2}.$$

Hence

$$\tau_2 = \frac{4}{v} \int_0^{\lambda_M} \frac{ds}{(1 - B/B_M)^{1/2}}.$$

Hamlin, Karplus, Vik and Watson (1961) have reduced (1.17) to the form

$$\tau_2 = \frac{4r_0}{v} T(\alpha_0).$$

The dimensionless function  $T(\alpha_0)$  increases monotonically from a value of 0.74 at  $\alpha_0 = \frac{1}{2} \pi$  to 1.38 at  $\alpha_0 = 0$  and is approximated by  $T(\alpha_0) \approx 1.30 - 0.56 \sin \alpha_0$ . For the geomagnetic field

$$\tau_2 = 0.085 (r_0/\beta) T(\alpha_0) \text{ seconds,}$$

with  $r_0$  (in Earth radii) being the equatorial radius of the line of force along which the guiding center oscillates.

Some representative values of  $\tau_2$  are given in Table 1.2.

**Table 1.2. Period of Latitudinal Oscillation,  $\tau_2$  for  $r_0 = 2.0$  Earth radii and  $\alpha_0 = \frac{1}{2} \pi$**

Particle	Kinetic Energy	$\beta$	$\tau_2$
Electron	10 kev	0.195	0.64 seconds
	100 kev	0.548	0.23
	1 Mev	0.941	0.13
Proton	10 kev	$4.61 \times 10^{-3}$	27.3
	100 kev	$1.46 \times 10^{-2}$	8.6
	1 Mev	$4.61 \times 10^{-2}$	2.7
	10 Mev	0.146	0.86
	100 Mev	0.428	0.29
	1 Bev	0.875	0.14

In addition to the oscillatory motion of the guiding center from one hemisphere to the other, there is a drift in longitude of the guiding center due to the inhomogeneity of the field and to the centrifugal force on the guiding center as it moves along the curved lines of force. The drift rate is a fluctuating function of time but is always in the same sense. The sense is opposite for particles of opposite sign. In the Earth's field, electrons drift toward the east, protons toward the west.

The drift velocity has been obtained by Alfvén and has been discussed further by Spitzer (1956), by Welch and Whitaker (1959), by Northrup and Teller (1960), by Hamlin, Karplus, Vik and Watson (1961) and by Lew (1961). The latter author has put the results into particularly convenient form. The time  $\tau_3$  required for one complete drift around the Earth is given by Lew as:

$$\tau_3 = 172.4 \frac{1 + \epsilon}{\epsilon(2 + \epsilon)} \frac{1}{m r_0} \frac{G}{F} \text{ minutes.} \tag{1.17}$$

In (1.17)  $\epsilon = (1 - \beta^2)^{-\frac{1}{2}} - 1$  is the ratio of kinetic energy of the particle to its rest energy,  $m$  is the rest mass of the particle in units of the rest mass of the electron,  $r_0$  is the equatorial radius of the line of force along which the guiding center is moving in units of the Earth's radius and  $G/F$  is the ratio of the drift period of particles mirroring at  $\lambda_M$  to that for particles mirroring at  $\lambda_M = 0$ .  $G/F$  is of the order of unity and is a function of  $\lambda_M$  only. It is tabulated in Table 1.3 and plotted in Figure 1.2.

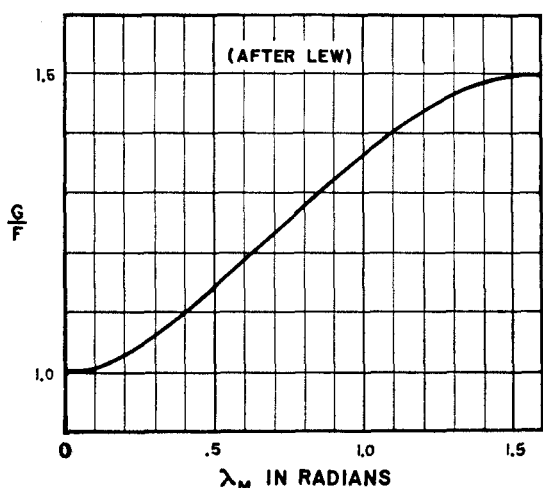


Fig. 1.2. The function  $G/F$  (after Lew) vs. mirror latitude used with Figure 1.3 in finding the longitudinal drift function.

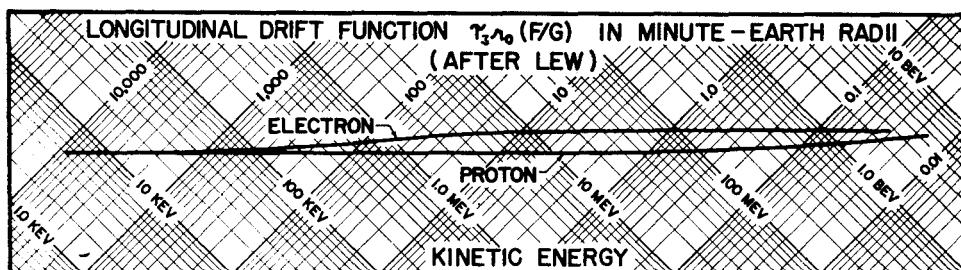


Fig. 1.3 A diagram for finding the longitudinal drift period  $\tau_3$  for electrons and protons of various energies on magnetic shells cutting the equator at radial distance  $r_0$ .

Figure 1.3 shows the 'longitudinal drift function'  $r_0 \tau_3 F/G$  as a function of kinetic energy for electrons and protons. As remarked by Lew, the longitudinal drift period for an electron is

always greater than that for a proton of the same kinetic energy but never more than by a factor of two.

**Table 1.3. (after J. S. Lew)**

$\lambda_M$	$G/F$	$\lambda_M$	$G/F$
radians		radians	
0.0	1.000	1.0	1.366
0.1	1.007	1.1	1.406
0.2	1.028	1.2	1.440
0.3	1.060	1.3	1.467
0.4	1.098	1.4	1.487
0.5	1.141	1.5	1.498
0.6	1.186	$\frac{1}{2}\pi$	1.500
0.7	1.232		
0.8	1.278		
0.9	1.323		

**1.4 LARMOR RADII OF TRAPPED PARTICLES**

It is often convenient in considering perturbations of trapped particles to have ready reference to the magnitudes of Larmor radii of protons and electrons of various energies in the Earth's field. Hence a brief summary is included in this section. It follows from equation (1.1) that

$$\rho = \frac{p_{\perp}c}{eB} = \frac{pc \sin \alpha}{eB}, \tag{1.18}$$

with  $e$  in electrostatic units,  $pc$  in ergs,  $\rho$  in centimeters and  $B$  in gauss. For a given momentum particle,  $\rho$  is proportional to  $\sin \alpha$ .

For the purposes of obtaining representative numerical values, equation (1.18) is specialized to the geomagnetic equator and to  $\alpha = \frac{1}{2}\pi$ :

$$\rho = 107.0 r_0^3 pc \text{ meters} \tag{1.19}$$

In (1.19)  $r_0$  is measured in Earth radii and  $pc$  in Mev. Sample values are given in Table 1.4.

**Table 1.4. Radii of Curvature in Earth's Field**

( $\lambda = 0, \alpha = \frac{1}{2}\pi, r_0 = 2.0$ )

Particle	Kinetic Energy	$pc$	$\rho$
Electron	10 kev	0.102 Mev	87 meters
	100 kev	0.335 Mev	287 meters
	1 Mev	1.422 Mev	1.22 km
Proton	10 kev	4.33 Mev	3.71 km
	100 kev	13.70 Mev	11.7 km
	1 Mev	43.3 Mev	37.1 km
	10 Mev	137.4 Mev	118 km
	100 Mev	444.5 Mev	381 km
	1 Bev	1695 Mev	1451 km

2.1 THE ROLE OF ADIABATIC INVARIANTS IN GEOMAGNETIC TRAPPING

There are three adiabatic invariants of trapped particle motion associated respectively with the three classes of cyclic motion discussed above.

The first is the Alfvén magnetic moment  $\mu$ . A special consequence of the conservation of  $\mu$  is that the locus of the mirror points of a particle's motion lies on a surface of constant scalar  $B$  ( $= B_M$ ).

The second is often called the longitudinal integral invariant. It is the action integral of the oscillating motion of the guiding center between mirror points, viz:

$$\mathcal{J} = \int_M^{M^*} p_{\parallel} ds, \tag{2.1}$$

the line integral being taken along the magnetic line of force between the mirror point  $M$  and its conjugate  $M^*$ . The conservation of  $\mathcal{J}$  was first recognized by Rosenbluth (Northrup and Teller, 1960). It is convenient to rewrite (2.1) as

$$\mathcal{J} = p \int_M^{M^*} (1 - B/B_M)^{\frac{1}{2}} ds$$

and to let

$$I = \frac{\mathcal{J}}{p} = \int_M^{M^*} (1 - B/B_M)^{\frac{1}{2}} ds. \tag{2.2}$$

The quantity  $I$  has the dimensions of length, is a property of the magnetic field alone and may be attributed to the mirror point  $M$  (or  $M^*$ ). The Rosenbluth principle for the conservation of  $I$  makes possible the identification of a unique sequence of segments of magnetic lines of force that constitute a single valued, three dimensional surface (a 'magnetic shell') on which the guiding center of a trapped particle will forever lie—to the extent that the conditions for the conservation of  $\mu$  and  $I$  are met—as it moves about in the irregular geomagnetic field.

The conservation of  $I$  is essential to the understanding of trapping in the real, irregular geomagnetic field, which does not possess axial symmetry and for which the Störmer first integral does not exist. The argument is illustrated in Figure 2.1. Let the surface  $B = \text{constant}$  shown there contain the locus of mirror points for a given particle. Let the motion of the particle's guiding center at a chosen time be along the line of force shown in the right-hand side of the figure with the integral  $I$  having the value  $I_0$ . The question then is: 'Along which of the infinite number of segments of lines of force having values of  $I - I_0, I_1, I_2$ , etc. (sketched in the left-hand side of Figure 2.1)—and having mirror points on the specified surface of constant  $B$ , will the guiding center of the particle be moving at some later time after a drift in longitude has occurred?' The Rosenbluth principle assures that it will be the segment characterized by  $I_0$ .

It is presumed that  $I$  ceases to be conserved when there are perturbations in the guiding magnetic field on a time-scale comparable to the period  $\tau_2$ . Typical, pertinent values of  $\tau_2$  are of the order of a fraction of a second. As in the case of the conservation of  $\mu$  there is no satisfactory quantitative foundation for calculating the rate of change of  $I$  under specified circumstances.

The third, and weakest, of the adiabatic invariants is the flux invariant  $\Phi$ . (Northrup and Teller, 1960).  $\Phi$  is the total flux of  $\mathbf{B}$  through a surface bounded by a magnetic shell as defined by  $I = \text{constant}$ . (The computation is made by considering flux in one sense only through the surface). Northrup and Teller show that  $d\Phi/dt = 0$  if the magnetic field within the region in question does not change significantly during  $\tau_3$ . It is seen from Figure 1.3 that  $\tau_3$  varies over a wide range for electrons and protons of typical energies—say from several

minutes to several days. Hence under actual geophysical circumstances it will not be surprising if  $\Phi$  is not conserved even though both  $I$  and  $\mu$  may be. Moreover, it appears that the non-conservation of  $\Phi$  is strongly dependent on particle energy.

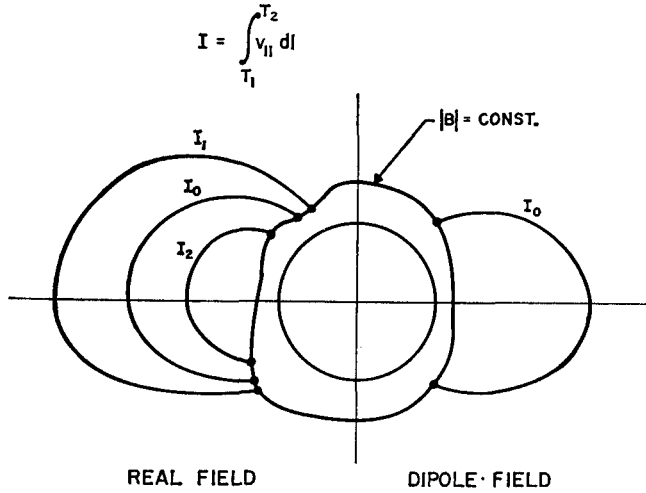


Fig. 2.1. Illustrating the principles of the conservation of the adiabatic invariants  $\mu$  and  $I$  in the geomagnetic field.

The magnitude of  $\tau_3$  also gives one a measure of the extent to which a lack of axial symmetry may be expected under time-varying conditions. (Welch and Whitaker, (1959)). For example, if a quantity of electrons having various energies of the order of 100 keV be injected into the field at  $r_0 = 3$  Earth radii,  $\tau_3 \approx 3$  hours and a time of the order of one day will be required for the establishment of axial symmetry.

In general summary it is clear that the theory associated with the three adiabatic invariants  $\mu$ ,  $I$  and  $\Phi$  and the three corresponding cyclic periods  $\tau_1$ ,  $\tau_2$  and  $\tau_3$  is essential to understanding not only

- (a) the time-stationary trapping situation, but also
- (b) any proposed time-dependent or spatially-dependent perturbation in the real geophysical situation.

2.2 THE NATURAL SYSTEM OF CO-ORDINATES FOR GEOMAGNETICALLY-TRAPPED PARTICLES

One of the problems in the study of the energetic particles which are trapped temporarily in the Earth's magnetic field is to identify the types of particles present, to measure the absolute energy spectrum of each type, and to make such determinations as a function of positional co-ordinates, of direction and of time.

The problem may be formulated succinctly with the help of the following symbols:

- $j_i$  —the uni-directional intensity of particles of type  $i$  having energies in  $dE$  at  $E$ .
- $r, \phi, \theta$  —the geographic polar co-ordinates of an arbitrary point in the vicinity of the Earth.
- $l, m, n$  —the direction cosines of the direction in space being considered.
- $E$  —particle kinetic energy.
- $t$  —time.

Thus, the problem may be said to be the determination of the functions

$$j_i(r, \phi, \theta, l, m, n, E, t)$$

where  $i$  denotes successively electrons, protons, alpha particles, etc.

The observational task which corresponds directly to this naive formulation of the problem is far beyond human capability. Fortunately, in a time-stationary state the application of the foregoing trapping theory simplifies the observational enterprise immensely, viz:

(a) At any point the physical situation possesses cylindrical symmetry about the magnetic field vector  $\mathbf{B}$  and mirror symmetry with respect to the plane perpendicular to  $\mathbf{B}$ . Thus all directions which make an angle  $\alpha$  (or  $180^\circ - \alpha$ ) with the magnetic field vector  $\mathbf{B}$  at a specified point are equivalent.

(b) Within a given geomagnetic shell as defined by the integral adiabatic invariant  $I$  and as labeled by a single parameter  $L$  (see later section), the complete positional and angular dependence of  $j_i$  is contained within the dependence of  $j_i$  on the angle  $\alpha_0$  to the  $\mathbf{B}$  vector at the position within the shell at which  $\mathbf{B}$  has its minimum value (loosely speaking, on the magnetic equator).

Hence the complete observational problem for the time-stationary state is reduced to that of determining

$$j_i(L, \alpha_0, E)$$

Within the physical limitations of their applicability, the two adiabatic invariants  $\mu$  and  $I$  provide a 'natural' system of geomagnetic co-ordinates which is suitable for the collation and comparison of observational data from a wide variety of geographic positions. This system of co-ordinates makes feasible the comprehensive study of large masses of data obtained under quiescent conditions; and, by the same token, it provides the proper foundation for studying time fluctuations.

In a quiescent, unperturbed case of magnetic trapping all particles which mirror on a given surface  $B = \text{constant}$  will always continue to do so; also the uni-directional intensity within a given magnetic shell  $j_i(B, \alpha_0)$  is independent of the magnitude and direction of  $\text{grad } B$ . Moreover their orbits drift around the Earth on such a sequence of lines of force as to conserve  $I$ . As mentioned above this latter principle defines a unique sequence of lines of force comprising a magnetic shell. The  $B, I$  co-ordinate system is relatively trivial for an idealized dipole. Nonetheless it is instructive to see the form of the surfaces  $B = \text{constant}$  and  $I = \text{constant}$  for a dipole. Several cases are illustrated in Figure 2.2. The  $B = \text{constant}$  and  $I = \text{constant}$  surfaces intersect in a system of small circles of various radii with their centers on the dipole axis. Each pair of such surfaces intersects in two such small circles, located respectively in opposite hemispheres.

For a dipole field it is readily shown that

$$I_M = L_M g(\lambda_M), \tag{2.3}$$

where the subscript M refers to quantities pertaining to a given mirror point;  $\lambda_M$  is the latitude of that mirror point;  $L_M$  is the radial distance at which the line of force through the mirror point crosses the equator;  $I_M$  is the value of the integral adiabatic invariant corresponding to the mirror point; and  $g$  is a function which is known explicitly (numerically but not in closed analytical form).

Also

$$\frac{(B_M)}{(B_M)_0} = \frac{(4 - 3 \cos^2 \lambda_M)^{\frac{1}{2}}}{\cos^6 \lambda_M}, \tag{2.4}$$

wherein  $(B_M)_0$  is the equatorial value of  $B$  on the line of force through the mirror point designated by  $M$ .

Following McIlwain (1960), it is found from (2.3) and (2.4) that

$$L_M^3 B_M = f(I_M^3 B_M) \quad (2.5)$$

In (2.5)  $f$  is a function which has been calculated numerically.

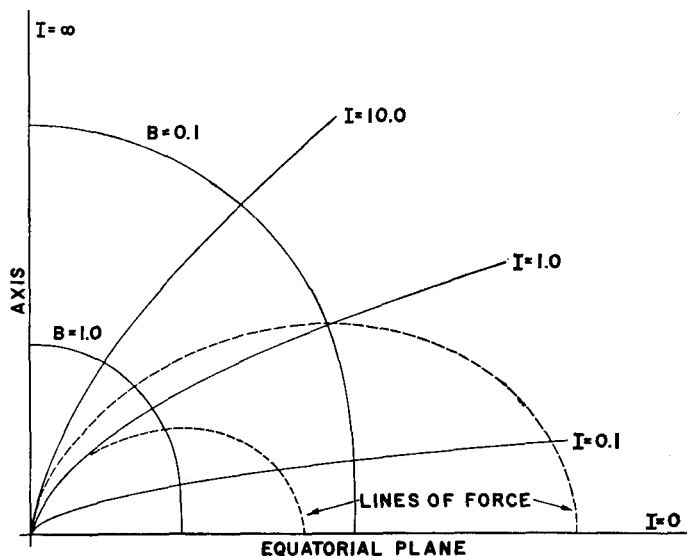


Fig. 2.2. The 'natural co-ordinate system' for trapped particles in an idealized dipole field showing contours of  $L = \text{constant}$ ,  $B = \text{constant}$  and  $I = \text{constant}$ .

For the real geomagnetic field, Jensen, Murray and Welch (1960), Vestine (1960) and Vestine and Sibley (1960) have calculated extensive numerical tables of  $B$  and  $I$  as a function of geographic co-ordinates around the Earth; they have also calculated a large number of lines of force in space. McIlwain (1960) and Ray (1960) have fitted functions of geographic co-ordinates to these numerical tables in forms which are convenient for machine-computer use in labeling the observations obtained with rocket, satellite and space probe equipment.

McIlwain has made a further important advance in the treatment of observational data by utilizing the dipole relation (2.5) to define a single parameter  $L$  to characterize a specific magnetic shell in its entirety. He has shown by numerical calculation on the real geomagnetic field that the 'shell parameter'  $L$  as so defined (using real field quantities in (2.5)) not only has the same simple (though approximate) physical meaning as for the dipole case but is indeed very nearly a constant along a given line of force over a large range of  $B_M$  and for all longitudes.

Hence there has now been adopted the co-ordinate system defined by surfaces of constant  $B$  and constant  $L$  in dealing with the huge body of observations on the geomagnetically trapped radiation. This co-ordinate system has a sound theoretical foundation and, in the hands of McIlwain, Pennington, Vestine, Forbush, Venkatesan, Ray, Welch, Lin, Pizzella, Van Allen and others, is proving of very great power in the study of trapped radiation in both quiescent and disturbed states. It makes possible the ready comparison of diverse observations at diverse points in space and it provides the foundation for the study of time fluctuations and for the discussion of a variety of theoretical aspects such as the lifetime of trapped particles, the consequences of local acceleration processes and the like.

2.3 APPLICATION OF LIOUVILLE'S THEOREM TO THE INTENSITY OF RADIATION TRAPPED IN THE GEOMAGNETIC FIELD

In an unpublished memorandum (1959) Ray has discussed the application of Liouville's theorem on the conservation of density of representative points in phase space to geomagnetically trapped particles. The following two theorems are representative examples of such application:

*Theorem 1.* If at any point on a particular line of force the directional intensity is isotropic, then along that line of force, in the direction of increasing magnetic field strength, at each point the radiation is isotropic and the omni-directional intensity is independent of position.

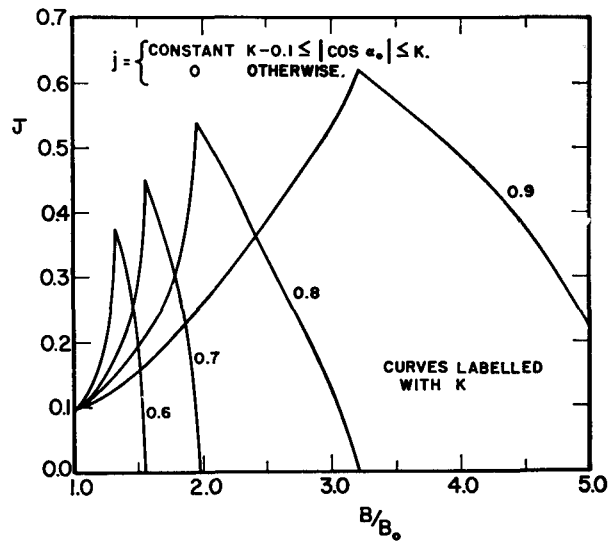


Fig. 2.3. Example of the relationship of angular distribution of uni-directional intensity  $j$  at the equator ( $B = B_0$ ) to the omni-directional intensity as a function of  $B/B_0$  for a given magnetic shell. (After E. C. Ray).

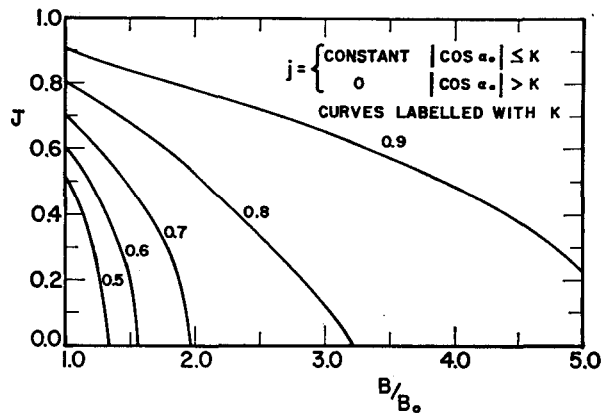


Fig. 2.4 Another example (after E. C. Ray).

*Theorem 2.* If, in a magnetic field in which the field strength increases as one goes along a line of force in the direction of decreasing radius  $r$ , the intensity has cylindrical symmetry about the line of force, and if the directional intensity at one point on a particular line of force increases (decreases) monotonically as the angle to the line of force decreases, the omnidirectional intensity increases (decreases) monotonically as one goes to lesser radii along the same line of force.

Ray (1960a) has also solved the following problem in an explicit form which has general applicability to the interpretation of experimental results:

Given: A complete knowledge of the omnidirectional intensity  $\mathcal{J}_0$  of a given type particle as a function of position (or equivalently as a function of  $B/B_0$ ) along a given line of force ( $L = \text{constant}$ ).

To find: The angular distribution of the uni-directional intensity  $j$  as a function of pitch angle  $\alpha_0$  at the equator,  $B/B_0 = 1$ .

Assuming the conservation of  $\mu$ , Ray finds:

$$j(h) = \frac{1}{2\pi^2} \frac{d}{dh} \int_0^h m^{\frac{1}{2}}(h-m)^{-\frac{1}{2}} \mathcal{J}_0(m) dm \quad (2.6)$$

where  $h$  is written for  $\sin^2\alpha_0$  and  $m$  for  $B_0/B$ .

#### 2.4 GENERAL REMARKS

It is now abundantly clear that the use of the system of 'natural co-ordinates' described above for the real geomagnetic field provides an immense simplification in interpreting experimental observations. In effect, the data for each magnetic shell (as specified by the parameter  $L$ ) are dealt with separately. And in fact, since the time-stationary situation has axial symmetry in  $B$ ,  $L$  co-ordinates, the physical situation along a single line of force of given  $L$  is taken to be representative of the entire shell to which it belongs. Within that shell  $\alpha_0$  (or if more convenient  $B$ , or  $B/B_0$  or  $\lambda_N = \text{arc sec}(L/r_N)^{\frac{1}{2}}$ ) is the only other parameter necessary for a complete specification of the positional and directional characteristics of the radiation.

In addition to aiding the interpretation of the quiescent state, the 'natural co-ordinates'  $B$  and  $L$  provide the proper basis for the clear recognition of temporal variations and for study of the detailed features of such variations. The SUI laboratory now routinely converts the geographic ephemerides of its various satellites to  $B$ ,  $L$  co-ordinates before attempting analysis.

#### 3.1 DISCOVERY OF THE GEOMAGNETICALLY-TRAPPED RADIATION

The previous sections have given a sketch of the dynamics of geomagnetically-trapped particles. Discussion is now directed to observational knowledge of the actual phenomena.

With the wisdom of retrospection it may well be said that since 1905, or thereabouts, it has been clear that it is physically possible for electrically charged particles to be temporarily trapped in the geomagnetic field. Moreover, the well-known phenomena of the aurorae and geomagnetic storms have led various workers, over the years, to conjecture on the existence of trapped particles. The ring-current hypothesis by Chapman and Ferraro (see Chapman and Bartels, 1940) was of this general nature as were the auroral theories of Alfvén (1950) and Martyn (1951). Large fluxes of electrons having energies in the range of tens of kev were directly observed by the author and his associates in 1952, 1953, 1954 and 1955 by rocket experiments in the Arctic (Van Allen, 1957) at altitudes of 60 to 110 kilometers and in 1957 by further rocket experiments in the Arctic and Antarctic. A similar but much smaller effect

of the same sort was observed by a Geiger tube in Sputnik II in early November 1957 (Vernov, Grigorov, Logachev, and Chudakov, 1958). It was later suggested by these workers that the effect was due to low-energy corpuscles arriving in bursts, presumably from the Sun. Meanwhile Singer (1957) had considered the motion of very low energy trapped electrons ( $E \sim 10$  ev) and protons ( $E \sim 20$  kev) according to the Alfvén theory and had suggested that the longitudinal drifts of these particles provided the microscopic foundation for the Chapman ring current. During late 1957 and early 1958 Christofilos called attention to the fact that the geomagnetic field would act as a temporary trap for the charged decay products of cosmic-ray-produced neutrons emerging from the atmosphere and he proposed a series of high-altitude atomic bomb bursts for the injection of energetic electrons into the geomagnetic field as an experimental test of this idea. He also gave a detailed theory of the rate of loss of trapped electrons into the atmosphere by multiple scattering. Unhappily all of this work of Christofilos was contained in classified documents and discussion of it was confined to a small segment of the scientific profession. Portions of it were released for publication considerably later (Christofilos, 1959), after successful conduct of the proposed experiments.

The first conclusive evidence for the existence of significant intensities of geomagnetically trapped particles was obtained by the author and his students by means of Geiger tubes flown in the U.S. satellites, Explorers I and III, in early 1958 (Van Allen, 1958), (Van Allen, Ludwig Ray and McIlwain, 1958). The data from these two satellites showed that in the latitude range  $\pm 30^\circ$ :

- (a) The intensity of radiation up to some 600 km altitude was in good accord with that to be expected for cosmic rays only, when proper account was taken of the increasing opening angles of geomagnetically allowed cones with increasing altitude and of the concurrent shrinking of the solid angle subtended at the observing point by the solid Earth (Kasper, 1960).
- (b) Above some 800 km (this transition altitude being longitude and latitude dependent) the intensity of radiation increased very rapidly with increasing altitude in a way totally inconsistent with cosmic ray expectations.
- (c) At the higher altitudes ( $\sim 2000$  km) the true counting rate of a Geiger tube with a geometric factor of  $17.4 \text{ cm}^2$  and with total shielding of about  $1.5 \text{ g/cm}^2$  of stainless steel (extrapolated range for electron of energy 3 Mev or range for protons of 30 Mev or  $1/e$  transmission for 75 kev X-rays) exceeded 25 000 counts per second. Hence the omni-directional intensity exceeded  $1700 \text{ (cm}^2\text{sec)}^{-1}$  if the radiation consisted wholly of penetrating particles; or it exceeded some  $10^8 \text{ (cm}^2\text{sec)}^{-1}$  if the radiation consisted wholly of electrons whose range was less than  $1.5 \text{ g/cm}^2$  but whose bremsstrahlung was sufficiently energetic to penetrate the absorber with little attenuation.

These observations were interpreted by the author (Van Allen, 1958) as conclusive evidence for the existence of large intensities of geomagnetically-trapped, electrically-charged particles, on the following grounds:

- (a) The amount of atmosphere surmounted in the altitude range say 600 to 1200 km was less by many orders of magnitude than the wall thickness of the counter. Hence the great increase in intensity with increasing altitude could not have been due to the progressive decrease of atmospheric absorption but must have been due to mechanical constraint of the radiation—specifically by the geomagnetic field. Hence the primary radiation being detected must have consisted of electrically-charged particles.
- (b) The charged particles in question could not have been coming from a source remote from the Earth by direct Störmer trajectories. For it would have required an inconceivably well-adjusted particle momentum to have produced this altitude dependence even at a

single latitude; and even if this had been so at, say, the equator, the particles arriving at slightly higher latitudes would have reached down to much lower altitudes—contrary to the observations.

(c) It was also regarded as quantitatively inconceivable that the radiation being detected was arriving directly from a distant source (e.g., the Sun) and was penetrating so deeply into the geomagnetic field near the equator in the form of neutral, ionized gas; and even if it were that it would be doing so at a rate which was independent of time.

### 3.2 THE SCOPE OF OBSERVATIONAL STUDY OF THE GEOMAGNETICALLY-TRAPPED RADIATION

The general nature of the observed results of the Iowa group was soon confirmed by two types of apparatus in Sputnik III, which was launched on 15 May 1958. One piece of apparatus was a shielded, cylindrical Na I scintillation crystal (40 by 39 mm in size) mounted on a photo-multiplier tube. The counting rate of pulses corresponding to energy loss greater than 35 keV was telemetered, as was also the quasi-d.c. current to the anode and to the 7th dynode of the photo-multiplier tube (Vernov, Vakulov, Gorchakov, Logachev and Chudakov, 1958). The second set of apparatus comprised two thin ZnS (Ag actuated) (thickness 2 mg/cm<sup>2</sup>) fluorescent screens covered with aluminum foils of thickness 0.8 and 0.4 mg/cm<sup>2</sup> respectively and also mounted on photo-multiplier tubes. (Krassovsky, Shklovsky, Galperin and Svetlitskiy, 1959). The inclination of the orbit of Sputnik III was 65° and the initial altitudes of perigee and apogee were 217 and 1878 km, respectively. The high intensity of radiation in the equatorial region was confirmed, a stripe of radiation in excess of the cosmic ray level was traversed in sub-auroral latitudes, and absolute intensities of a tentative nature were presented. The first American satellite to carry a system of radiation detectors designed with prior knowledge of the existence and approximate intensity and nature of the trapped radiation was Explorer IV, launched on 26 July 1958 into a 51° inclination orbit with initial perigee and apogee altitudes of 262 and 2210 kilometers. The apparatus designed and built by the Iowa group comprised two small Geiger tubes having different shielding, a small disk of plastic scintillator on a photo-multiplier tube for pulse counting and a small Cs I detector, covered by a 1 mg/cm<sup>2</sup> foil and also mounted on a photo-multiplier tube for energy flux measurement. This apparatus operated for about eight weeks and yielded an enormous amount of data as recorded on over 4000 passes by a world-wide network of receiving stations. Much of the data is still under study though several major papers have been published. (Van Allen, McIlwain and Ludwig 1959, 1959a), (McIlwain and Rothwell, 1959), (Ray, 1960), (Rothwell and McIlwain, 1959), Rothwell and McIlwain, 1960), (McIlwain, 1961). Subsequent U.S. satellites and space probes which have been devoted in part at least to study of the geomagnetically trapped radiation are the following, with launching data in parentheses: Explorer VI (7 August 1959); Explorer VII (13 October 1959); Injun (29 June 1961); Pioneer I (11 October 1958); Pioneer II (8 November 1958); Pioneer III (6 December 1958); Pioneer IV (3 March 1959); Pioneer V (11 March 1960); and a variety of smaller rockets and auxiliary scientific packages carried by military test rockets. Packages of emulsions on some of the flights in the latter category have been recovered. The longest term series of observation is that by Explorer VII; some 1 500 000 workable data points have been obtained over a sixteen month period. U.S.S.R. investigators have flown radiation measuring equipment on two deep space probes: Cosmic Rocket I (2 January 1959) and Cosmic Rocket II (2 September 1959), but have not reported any further satellite measurements in this field since Sputnik III (15 May 1958).

Thus, there is now a large body of observational knowledge concerning energetic corpuscular radiation around the Earth, obtained with a diversity of techniques. The following sections give a brief summary of what is known about various aspects.

3.3 GEOMETRIC STRUCTURE

For the present purpose the term 'geometric structure' or simply 'structure' is taken to mean the spatial distribution of the omni-directional intensity of a specified component of the trapped radiation. Inasmuch as the radiation is a mixture of protons and electrons (and perhaps other particles) having separate energy spectra which are quite different from each other and which are a function of  $L$ , of  $\alpha_0$  and of  $t$ , it is necessary to investigate the structure with a variety of detectors of different properties. *A priori*, it might be thought that the structures for different components might be very much different. But in fact there are certain powerful factors of a general nature which greatly reduce the conceivable variety of structures. The factors are as follows:

- (a) The dominance of the geomagnetic field in controlling the general form of the structure.
- (b) The dominance of atmospheric scattering and absorption in determining the form of the inner boundary of the intensity structure, near the Earth.
- (c) The nature of the process of injection of solar gas into the outer portion of the geomagnetic field and the nature of the subsequent 'local acceleration' processes.
- (d) The geometric character of the injection of particles from 'internal' sources.

In fact a single diagram is found to serve for the purpose of a general account of the subject of structure. Such a diagram was constructed by Van Allen and Frank (1959) on the basis of the extensive low-altitude satellite observations with the variety of detectors in Explorer IV and with the two traversals through the trapping region by Pioneer III. It is shown in Figure 3.1. On the basis of more recent data of Explorers VI and VII to be given later, it appears

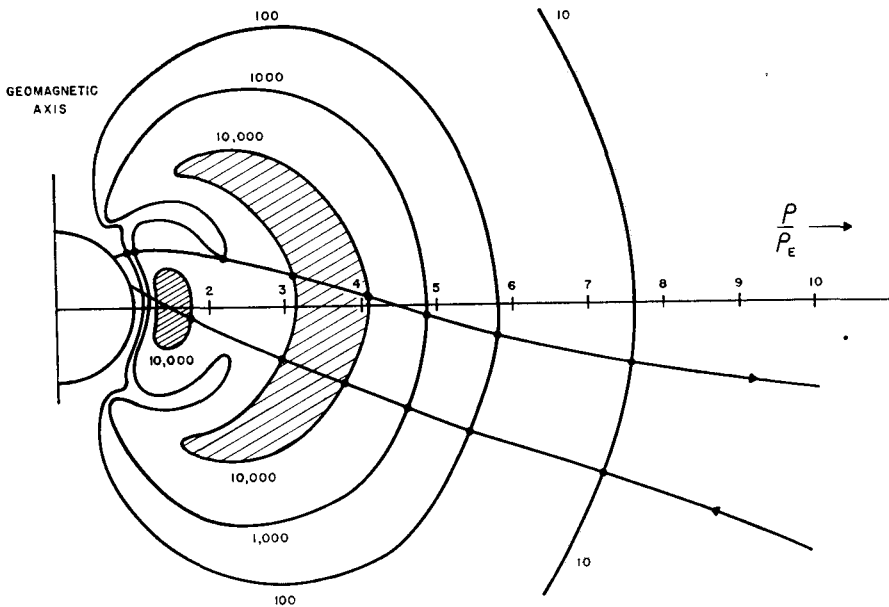


Fig. 3.1. Original diagram of the intensity structure of the trapped radiation around the Earth. The diagram is a section in a geomagnetic meridian plane of a three-dimensional figure of revolution around the geomagnetic axis. Contours of intensity are labeled with numbers, 10, 100, 1000, 10 000. These numbers are the true counting rates of an Anton 302 Geiger tube carried by Explorer IV and Pioneer III. The linear scale of the diagram is relative to the radius of the Earth—6371 km. The outbound and inbound legs of the trajectory of Pioneer III are shown by the slanting, undulating lines (after Van Allen and Frank).

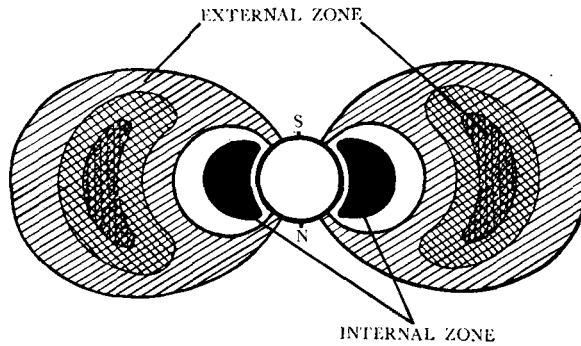


Fig. 3.2 A diagram of the same nature as Figure 3.1 (after Vernov and Chudakov).

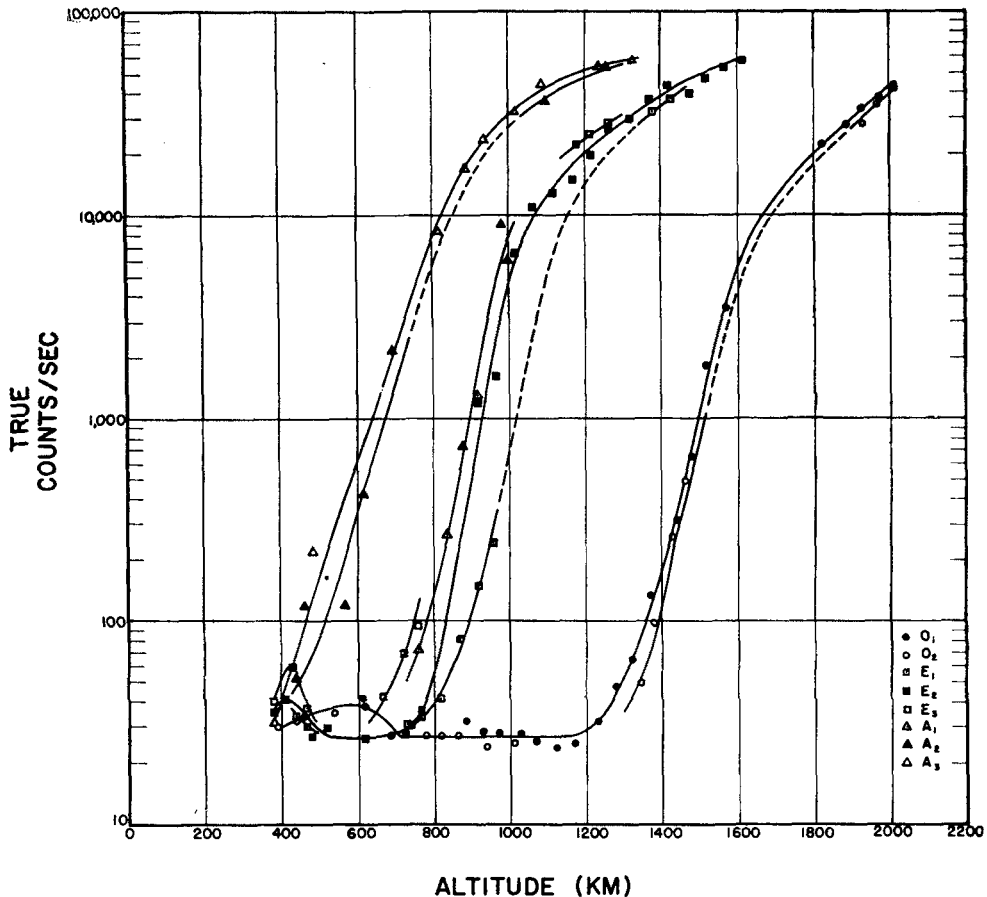


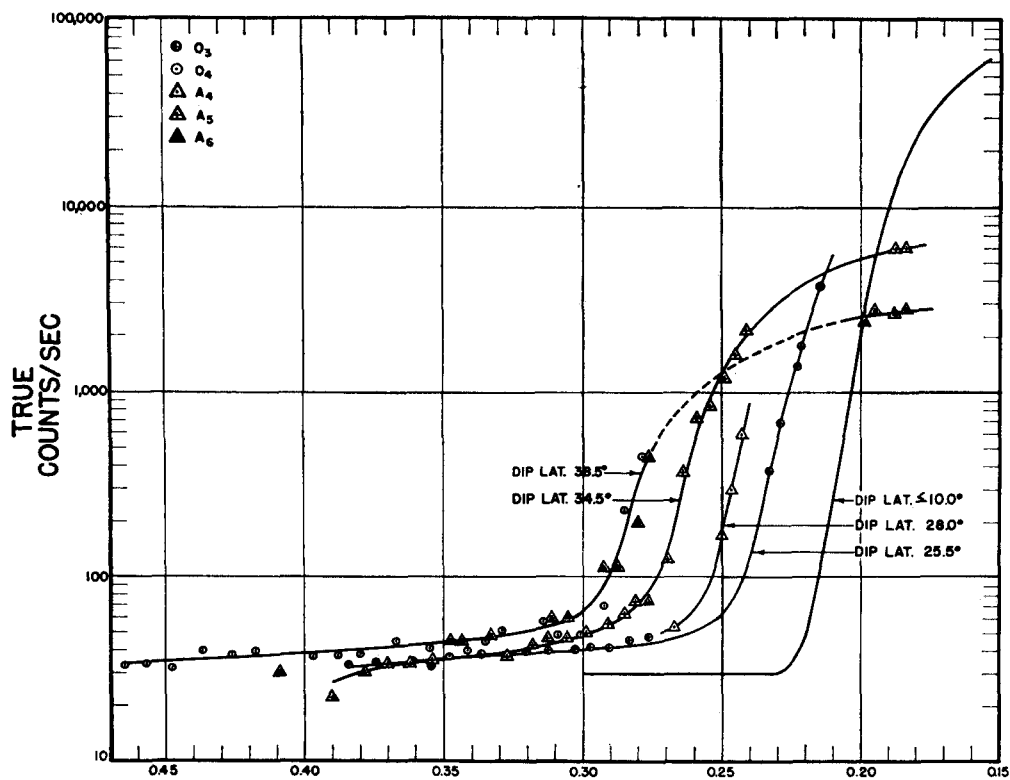
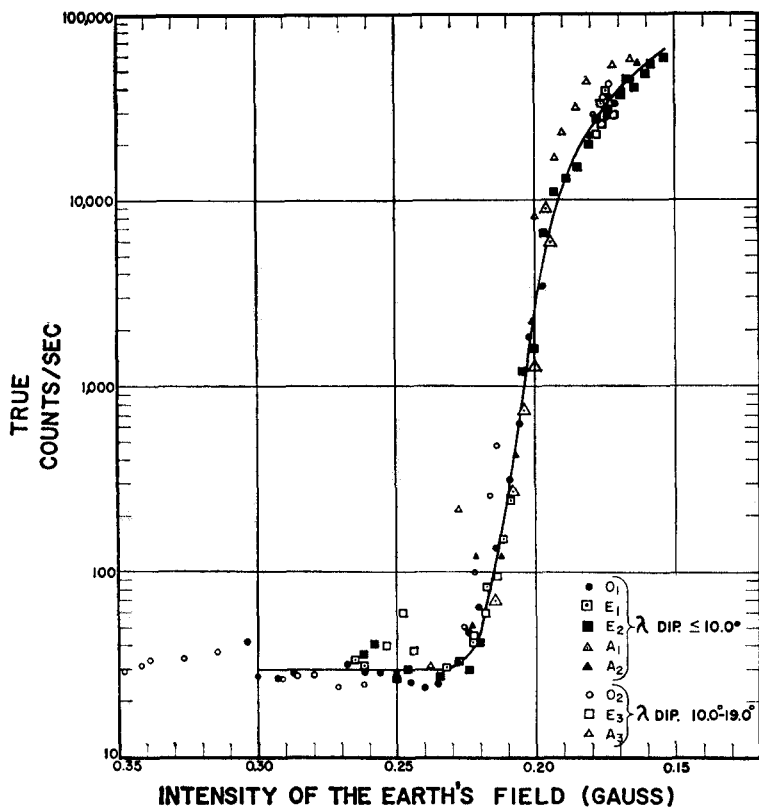
Fig. 3.3. True counting rate of the Geiger tube in Explorer I as a function of altitude above sea level for a number of geographic positions, all near the equator but at widely different longitudes. Note the precipitous rise in intensity beginning at an altitude ranging from 400 km. over the Central Atlantic (curve on the left) to 1300 km over Singapore (curve on the right). The effective eccentricity of the magnetic center of the Earth is obtained directly from the diagram. (After Yoshida, Ludwig and Van Allen).

Figures 3.4 and 3.5 are printed on the opposite page, 119; the legends are:

Fig. 3.4. The counting rate data of Figure 3.3 replotted as a function of scalar  $B$ . This diagram illustrates that the omni-directional intensity  $\mathcal{J}_0$  is a function only of  $B$  for  $I \approx \text{zero}$ . (After Yoshida, Ludwig, and Van Allen).

Fig. 3.5. Data similar to those in Figure 3.4 but for a variety of dip latitudes or magnetic shells. (After Yoshida, Ludwig, and Van Allen).

Figs. 3-4 and 3-5



that the form of the outer zone is more nearly like that of a dipole field than shown in Figure 3.1. The radiation region appears to be fundamentally divided into two distinct zones—an inner zone whose particle population is probably due to internal sources, located in the strong

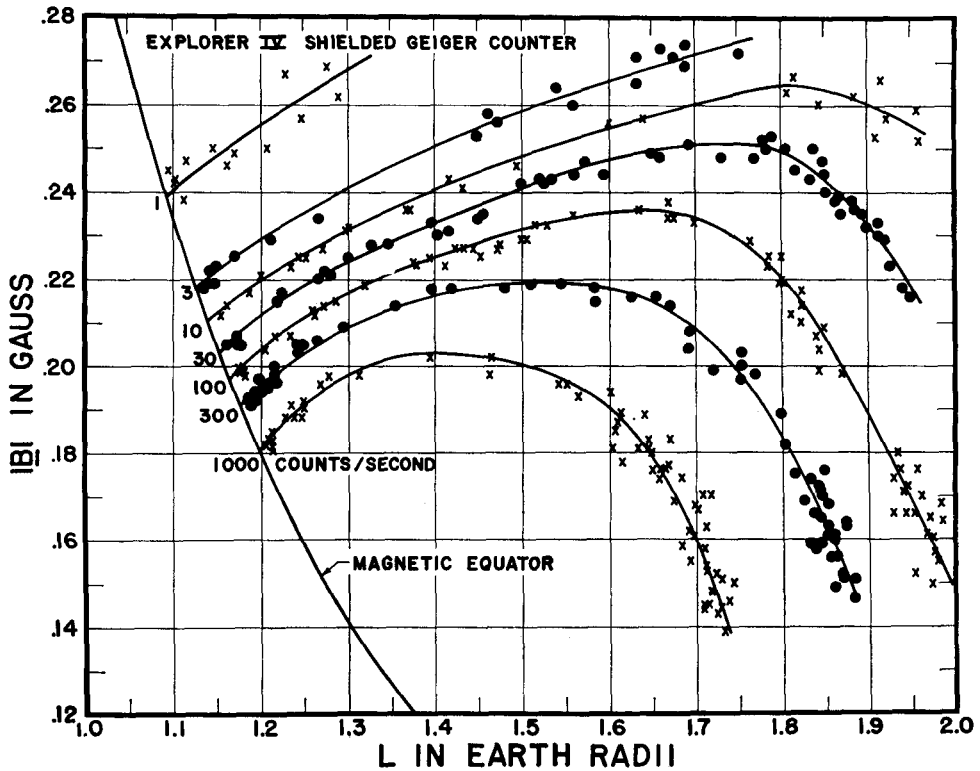


Fig. 3.6. Intensity contours on a  $B, L$  diagram of data from Explorer IV. Circles and crosses are used alternately to distinguish successive contours. (After McIlwain).

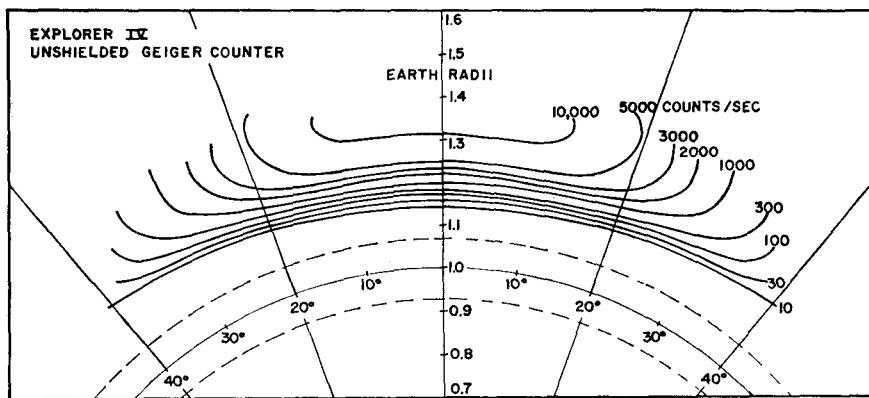


Fig. 3.8. Intensity contours of Figure 3.6 transformed to a spherical plot by using the co-ordinates  $r_N$  and  $\lambda_N$  defined from the natural co-ordinate system of  $B$  and  $L$ . The dashed arcs of circles represent the limits between which the surface of the solid Earth falls at various longitudes. (After McIlwain).

region of the geomagnetic field and relatively stable in time; and an outer zone, whose particle population is almost certainly due to external sources, located in the outer reaches of the geomagnetic field and having a detailed form and particle content which are strongly dependent on solar and geomagnetic activity as measured by other means. The region between the two zones has been termed the 'slot'.

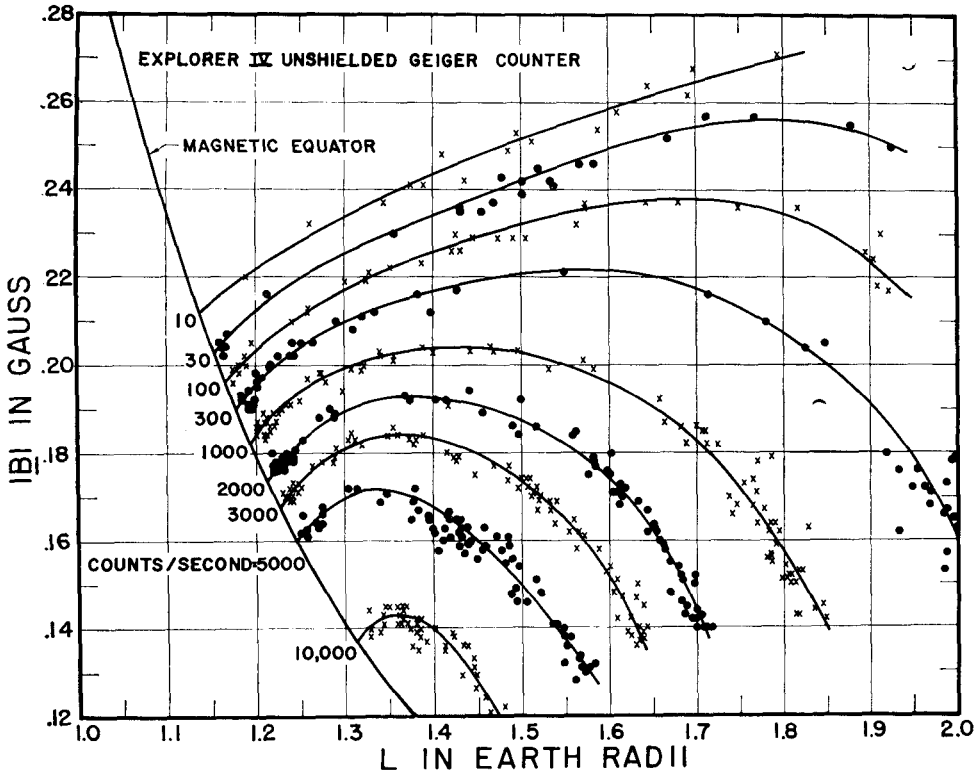


Fig. 3.7. Similar to Figure 3.6.

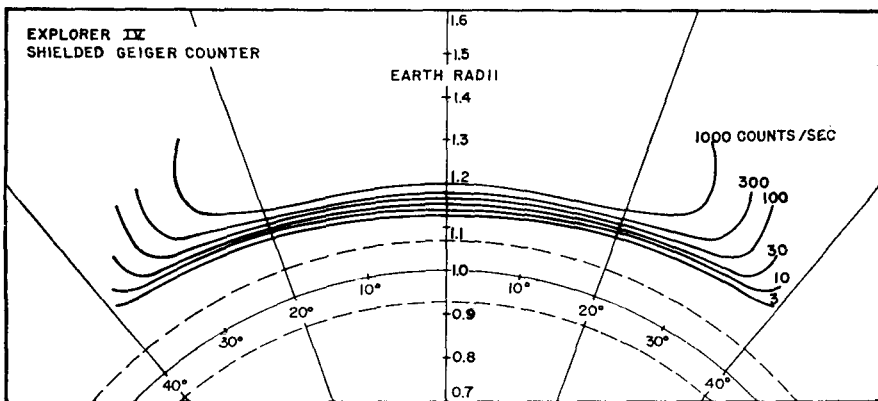


Fig. 3.9. Similar to Figure 3.8, showing the transformation of the contours of Figure 3.7.

A later version of the same sort of diagram by Vernov and Chudakov is shown in Figure 3.2.

The lower fringe of the inner zone was well determined by a single Geiger tube in Explorer I (Yoshida, Ludwig, and Van Allen, 1960). Figures 3.3, 3.4 and 3.5 summarize the main features of this work. The fact that the intensity data from all longitudes near the equator, for example, fall on a single curve when plotted against scalar  $B$  was one of the early successes of the  $B, L$  co-ordinate system described in detail in an earlier section.

The extensive undertaking of replotting in natural co-ordinates the inner zone data from the two Geiger tubes in Explorer IV has recently been completed by McIlwain (1961). Figures 3.6, 3.7, 3.8 and 3.9 show the principal results of this work. In the latter two figures, the radial and angular co-ordinates ( $r_N, \lambda_N$ ) are defined from the  $B, L$  system by the following two relations:

$$\lambda_N = \text{arc sec}(L/r_N)^{\frac{1}{2}} \quad (3.1)$$

$$B = \frac{M}{r_N^3} \left( 4 - \frac{3r_N}{L} \right)^{\frac{1}{2}} \quad (3.2)$$

(The unit of length is the radius of the Earth). The subscript  $N$  refers to the natural co-ordinate system and is intended to avoid confusion with any actual geometric co-ordinates.

The omni-directional intensity of protons in particles/cm<sup>2</sup>sec, trustworthy to a factor of two (during the period of the observations 26 July–21 September 1958), can be obtained as follows:

- (a) Divide the counting rate number given in the figures for the unshielded counter by 0.54 to obtain the omni-directional intensity of protons having energies exceeding 31 Mev;
- (b) Divide the counting rate number given in the figures for the shielded counter by 0.62 to obtain the omni-directional intensity of protons having energies exceeding 43 Mev.

A similar analysis is in progress on the observations with the other two detectors in Explorer IV: (a) the directional intensity of electrons of energy greater than 580 kev and (b) the directional energy flux into a thin CsI crystal covered with a 1 mg/cm<sup>2</sup> absorber. It is already apparent that the structure of the lower half of the inner zone for energetic electrons is similar to that for protons, though it spreads out to somewhat higher latitudes. The uni-directional intensity of electrons of energy greater than 580 kev in the direction perpendicular to  $B$  in the heart of the inner zone is  $1 \times 10^7$ /cm<sup>2</sup> sec steradian with an uncertainty of a factor of 2 ( $r_N \sim 1.4$  Earth radii).

The altitude dependence of proton intensity in the lower portion of the inner zone is, generally speaking, as well understood as knowledge of the density and composition of the atmosphere permits. The approximate argument is as follows. In the lower portion of the inner zone the dominant mechanisms for loss of particles are energy loss and scattering in the high levels of the atmosphere. Hence the intensity at a given value of  $B_M$  in a magnetic shell of given  $L$  is essentially inversely proportional to the line integral of atmospheric path length (in g/cm<sup>2</sup>) along the trajectory of the particle between  $B_M$  and  $B_{M*}$ , provided that the source function of particles is more or less the same over the region in question. This sort of analysis yields a substantially satisfactory understanding of the altitude dependence of intensity in the lower portion of the inner zone (Ray, 1960).

The fall-off of *both* electron and proton intensity with increasing radius (and the concomitant fall-off with increasing latitude) is not well understood. There is some contribution to the fall-off simply by the geometric dependence of the source function of albedo neutron decay products. But the observed fall-off is considerably more rapid than this.

Singer (1959, 1960) and Vernov (1960) have advocated the 'breakdown' of the Alfvén adiabatic invariant as a possible explanation and Singer has calculated what value of the Alfvén positional discriminant  $\rho|\text{grad } B/B|$  would be required to harmonize this line of thought with the observed data of the Iowa and Chicago groups. He finds a value of 0.08 to 0.06 as calculated in the equatorial plane.

The physical process which must be envisioned in the so-called breakdown of the adiabatic invariant is that the mirror point of a particle becomes progressively or randomly lower than that given by equation (1.13):

$$B_M = B_0/\sin^2 \alpha_0,$$

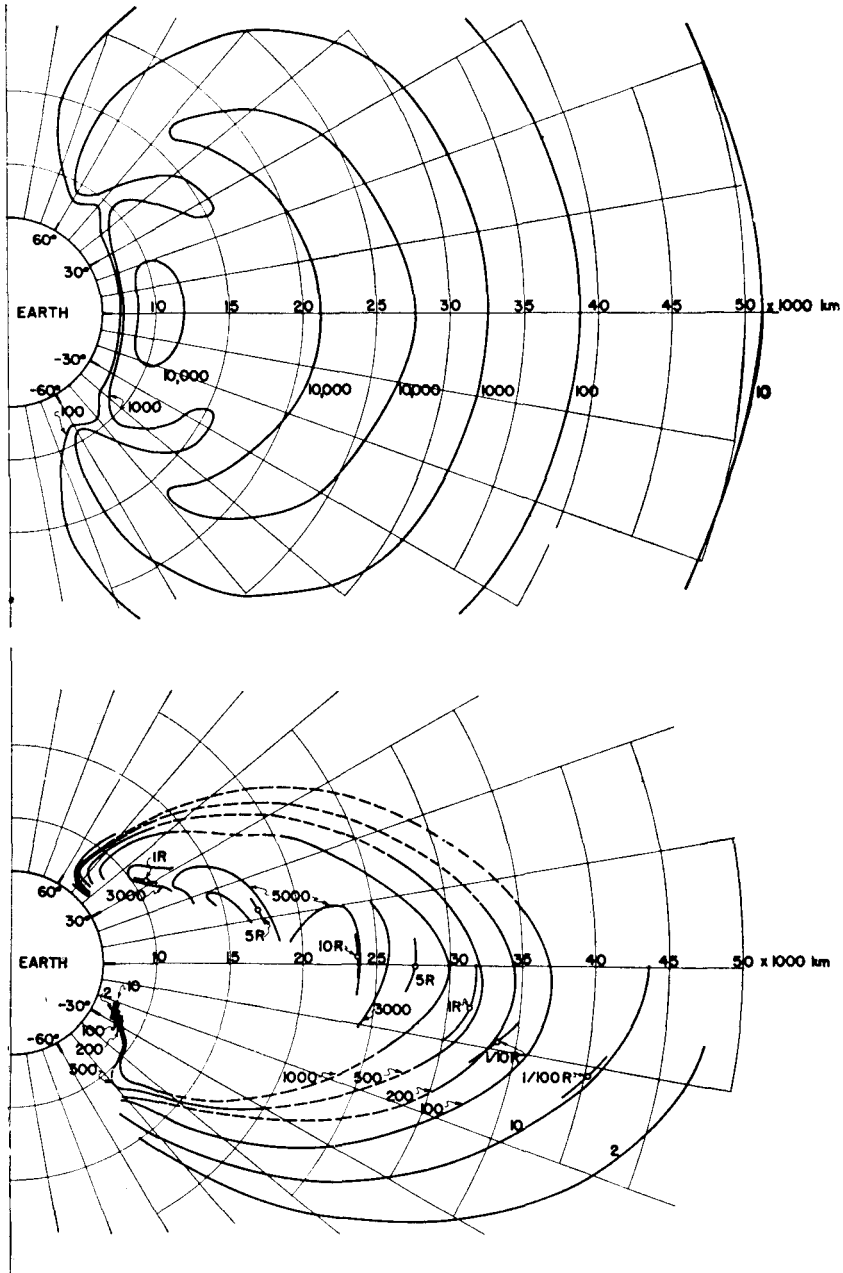
or that  $p_{\parallel}$  at the equator progressively or randomly increases at the expense of  $p_{\perp}$  so that  $\alpha_0$  diminishes. (See sections 1.2 and 1.3). In the experiments of Gibson *et al* previously cited, it was found that the quiescent loss of trapped particles due to breakdown of the adiabatic invariant was unobservably small for over  $10^8$  encounters with a magnetic mirror where  $\rho|\text{grad } B/B| \sim 0.02$ . The number of possible encounters may be very much greater. It is also of interest to note that for the Störmer case which has been used as an illustration in section 1.1 (Figure 1.1),  $pc = 966$  Mev,  $E = 400$  Mev for a proton,  $(r_1 + r_2)/2 = 2.69$  Earth radii and  $\rho|\text{grad } B/B| \sim 0.17$  in the vicinity of the mirror point and 0.35 in the equatorial plane.

There is little doubt of the qualitative soundness of the Singer-Vernov suggestion but it is far from clear that the loss of trapped protons from the outer edge of the inner zone is actually dominated by the quiescent loss process proposed. Additional doubt is cast on the proposal by the fact that the inner zone structure for electrons whose energy exceeds 580 kev is quite similar to that for protons whose energy exceeds 30 Mev, being extended in the equatorial plane by only about 0.3 of an Earth's radius. For example, the Alfvén discriminant for an electron of 1 Mev kinetic energy at a radial distance of 2.4 Earth radii in the equatorial plane is only  $4 \times 10^{-4}$ .

The present author is inclined to the view that the radial limitation of the inner zone is caused in a dominant way by transient variations both in time and space of the geomagnetic field. The observational evidence for this view is that the low altitude portion of the inner zone in the equatorial region is quite stable but that temporal variations increase as one goes to higher latitudes; and in the slot variations of over an order of magnitude are observed, often with sharp spatial and temporal structure.

Specific models of hydromagnetic wave perturbations in the inner zone have been proposed by Welch and Whitaker (1959), Dragt and Dessler (Dragt, 1960) and by Wentzel (1961). The latter two authors have developed the theory of the perturbations by hydromagnetic waves in quantitative detail and have demonstrated the plausibility of the observed radial extent of the inner zone for protons. Wentzel has also discussed the question of electrons and has concluded that during strong geomagnetic storms electron orbits may also be significantly perturbed. It is important to keep in mind the fact that the presumed source function for the inner zone is a very weak one and that particle life-times of the order of  $10^8$  seconds are required in order to permit the development of the observed intensities in the heart of the inner zone.

The structure of the outer zone as sampled by lightly shielded Geiger tubes has been shown in Figure 3.1. A considerably modified structure (Van Allen and Frank 1959a) was observed by an identical detector in Pioneer IV, thus providing a striking example of the great time variability of the structure. This variability had been found in the earlier low-altitude observations with Explorer IV (Rothwell and McIlwain, 1960).



Comparison of the counting rate contours in the radiation zone as given by Van Allen (upper) and as given by analysis of Explorer VI (lower) shown on a polar plot. It is apparent that the radiation zones during the time of Explorer VI have shrunk considerably and changed form since those inferred from the Explorer IV and Pioneer III and IV data.

Fig. 3.10. Intensity structure of radiation region (Upper diagram after Van Allen and Frank; lower diagram after Arnoldy, Hoffman and Winckler).

Much extended studies of the outer-zone variations have been made recently using low-altitude data of Explorer VII (Forbush, Venkatesan and McIlwain, 1961) and using the high-altitude data of the very eccentric orbit of Explorer VI (Arnoldy, Hoffman and Winckler,

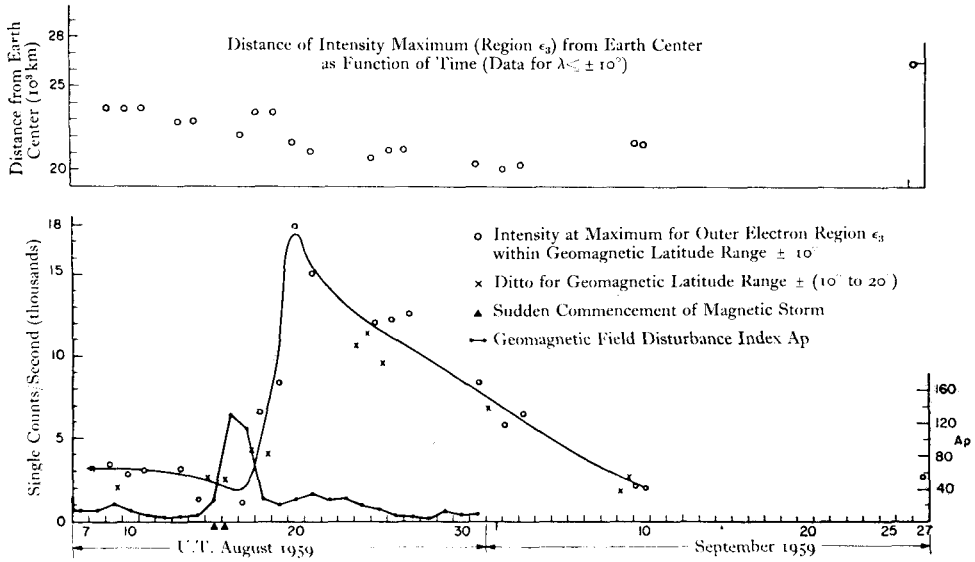


Fig. 3.11. A representation of time variations of intensity in the outer zone near the equatorial plane and relationship to magnetic activity (after Fan, Meyer, and Simpson).

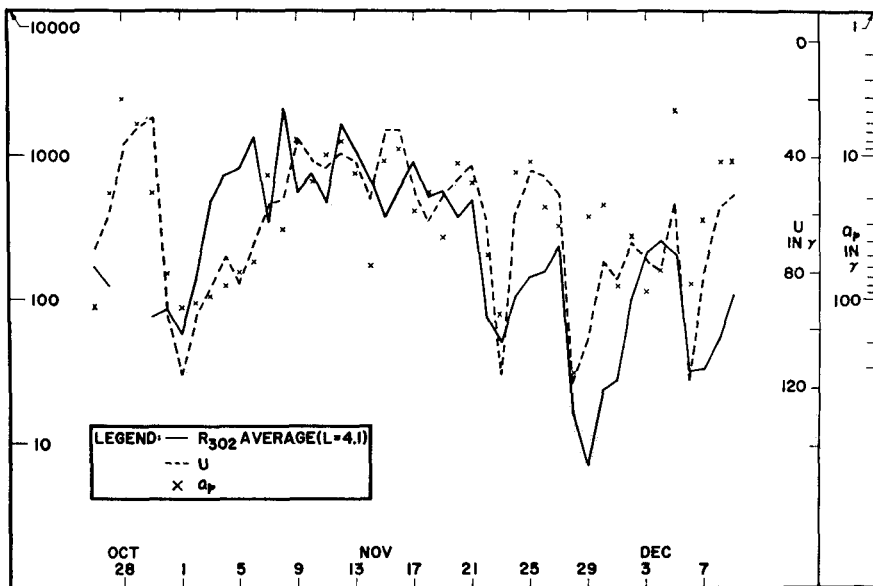


Fig. 3.12. Average counting rate,  $R_{302}$  at  $L = 4.1$  from passes for each 'day', equatorial ring current measure  $U$ , and magnetic activity  $a_p$ , 1959 October 26—December 9. A representation of time variations of intensity at about 1000 km altitude in the outer zone and relationship to magnetic activity. (After Forbush, Venkatesan, and McIlwain).

1960) (Fan, Meyer and Simpson, 1960), (Rosen and Farley, 1961). Figure 3.10 shows the structure of the outer zone during August-September 1959 as reported by Winckler *et al.* Figures 3.11 and 3.12 show examples of the time variation as measured in different ways. Forbush *et al* have found the geomagnetic ring current parameter of Kertz (1958) to be a valuable one in establishing a general connection between outer zone fluctuation and other geomagnetic effects. Fan *et al* have emphasized the bifurcation of the outer zone, as observed by Explorer VI to exist to varying degrees during August-September 1959, and as previously seen in Pioneer III data of December 1958 and have conjectured that this bifurcation is a characteristic feature of the outer zone. The low-altitude data of the Iowa group with Explorer VII show a strongly time-varying structure of the outer zone including many examples of double and multiple peaks. Hence, more extended observations of the outer zone structure as found at large radial distances will be required to find whether the August-September situation is characteristic or whether it merely represented a temporary one of a large variety of time-variable structural features.

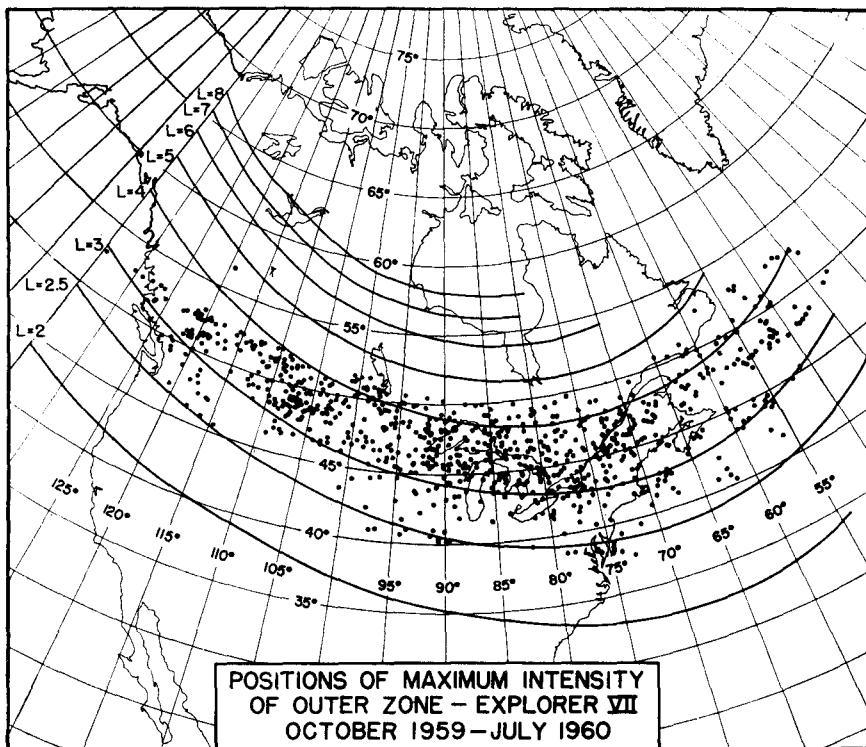


Fig. 3.13. Map of the geographic positions of the observed maximum intensity of the outer zone as projected along lines of force on to a sphere of radius 100 km greater than that of the Earth and corresponding loci of magnetic shells  $L = \text{constant}$  (after Lin and Van Allen).

Figure 3.13 shows a large collection of data (Lin and Van Allen, 1960) on the observed position of the peak intensity of the outer zone as found at  $\sim 1000$  kilometer altitude with Explorer VII. Also shown are the contours of  $L = \text{constant}$ . All of the data including the contours are with reference to a sphere of radius 100 km greater than that of the Earth. The mean position of the peak of the outer zone lies at an  $L$  of about 3.5 which is in remarkably close agreement with its location as found with Pioneer III near the equatorial plane.

Perhaps one of the most striking examples of the validity of present knowledge of the dynamics of geomagnetic trapping was provided by the Explorer IV observations of the artificially produced shells of energetic electrons from the Argus tests in August and Sept-

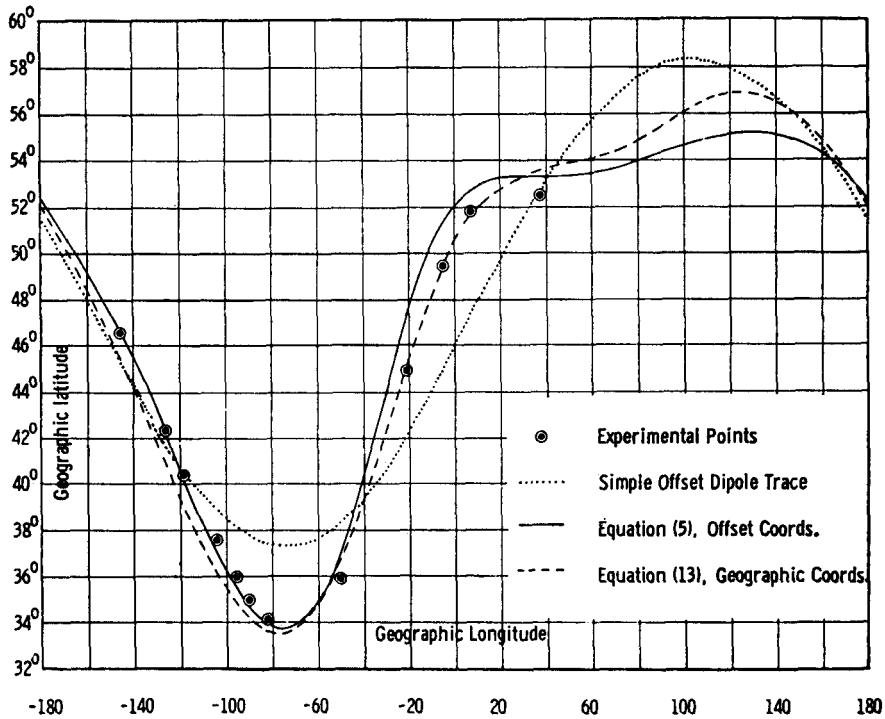


Fig. 3.14. Earth trace of Argus III shell. Various fits to the Argus III data of Explorer IV showing efficacy of the natural co-ordinate system (after Pennington).

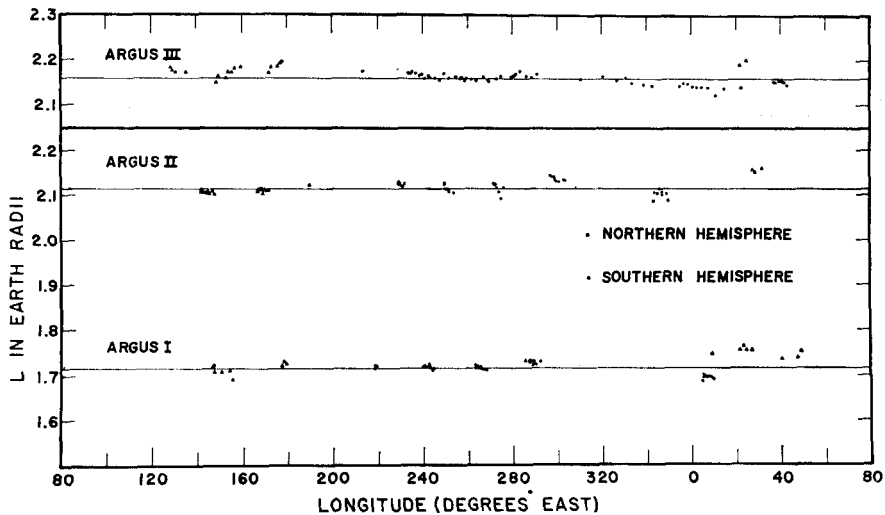


Fig. 3.15. The geomagnetic shell co-ordinate  $L$  of the three Argus shells as observed with Explorer IV as a function of geographic longitude (after McIlwain).

ember 1958. (Van Allen, McIlwain and Ludwig, 1959a), (Pennington, 1961), (McIlwain, 1961). Figures 3.14 and 3.15 show the remarkable agreement of the form of the three separate Argus shells with magnetic shells defined by  $L = \text{constant}$ .

#### 4.1 SOURCES OF TRAPPED PARTICLES IN THE INNER ZONE

In consideration of the gross intensity structure of the Earth's radiation region (See Figure 3.1) and of the quite different level of time variability in the inner and outer zones it seems reasonable to believe that the two zones originate in different ways.

It is now regarded as likely that the principal source of the particles which are trapped in the inner zone is the neutron component of the cosmic ray albedo arising from nuclear disintegrations produced in the atmosphere by the ordinary cosmic radiation.

The charged particle albedo of the atmosphere has long been recognized as a problem in the determination of the primary cosmic ray intensity by measurements with rocket equipment above the atmosphere (H. Kulenkampf, 1933), (Van Allen and Tatel, 1948), (Gangnes, Jenkins, and Van Allen, 1949), (Van Allen and Singer, 1950) and the neutron component has been discussed by Rossi (1948) as representing one of the losses from the atmosphere in assessing the energy integral of cosmic rays by summing all observable secondary processes.

The possible significance of the albedo neutrons for injecting their charged decay products into trapped orbits within the Earth's field was apparently first recognized by Christofilos (1958) whose attention was directed primarily to their decay electrons (beta ray spectrum with upper limit of 782 keV for a neutron at rest). Later more quantitative studies of this hypothesis were published by Singer (1958), by Vernov and Lebidinsky (1958) and by Kellogg (1959) after the experimental discovery of the trapped radiation. Singer's treatment of the problem concentrated on the proton decay products and Kellogg's on the electron decay products.

Later comprehensive treatments of the neutron albedo theory have come from the work of Hess and others. (Hess, 1959), (Hess and Starnes, 1960), (Hess, Canfield, and Lingenfelter, 1961), (Hess, Patterson, Wallace, and Chupp, 1959).

The data of Explorer IV and of Pioneer IV made it appear likely that the penetrating component in the inner zone was composed of protons (Van Allen, 1959). The first conclusive identification of this component was by way of recovered nuclear emulsions which had been flown through the lower edge of the inner zone by Freden and White (1959). Subsequent work by similar techniques by the same authors (Freden and White, 1960), by Yagoda (1960), by Armstrong, Harrison and Rosen (1959, 1960) and by Naugle and Kniffen (1961) have provided a good preliminary knowledge of the energy spectrum of protons in the lower portion of the inner zone. The differential number-energy spectrum is given by Freden and White (1959) as

$$j(E) dE = \kappa E^{-1.8} dE \quad (4.1)$$

for

$$75 < E < 700 \text{ Mev.}$$

The absolute source function for the injection of neutron decay products into the geomagnetic field (including angular distribution, spatial distribution and energy distribution of the decay products) is now rather well known, particularly by virtue of the work of Hess and his co-workers.

Also the theory of the loss of trapped protons from the range of detectability by energy loss and scattering in the tenuous upper atmosphere is as well known as are the properties of the exosphere (Ray, 1960). Hence it is possible to calculate the absolute intensities of trapped protons and their energy spectrum without reference to the experimental data. When this is done, there is a quite plausible measure of agreement with the observed quantities.

The corresponding situation with respect to the electrons in the inner zone is far less satisfactory (Kellogg, 1960). There are disagreements of orders of magnitude between the observed absolute intensities of electrons and the predicted values. Moreover the observed spectrum (Holly and Johnson, 1960) is relatively much richer in low-energy electrons than is the predicted spectrum. And, as remarked earlier, only the lower altitude (and low-latitude) portion of the structure of the inner zone is properly accounted for by the neutron albedo theory. Any proper understanding of the outer boundary of the inner zone must rest on other considerations.

It was found by Naugle and Kniffen (1961) that the proton spectrum at the northern edge of the inner zone in the energy range 10 to 50 Mev was very much steeper than that at a position some 1600 km south of this point, being of the form:

$$j(E)dE = \kappa' E^{-4.5} dE \quad (4.2)$$

It is perhaps significant that the rocket flight on which these results were obtained was on 19 September 1960, only about two weeks after the prolonged solar cosmic ray event of 3 to 10 September 1960. For some time the present author has entertained the thought that solar cosmic rays may make a significant contribution to the trapped proton content of the inner zone by way of neutron albedo secondaries produced in the polar caps. An effect suggestive of this possibility was reported by Armstrong *et al* (1961). Recently an important new development has occurred. Pizzella (1961) has found a marked increase in intensity in the inner zone following the early April 1960 solar cosmic ray events (Van Allen and Lin, 1961). The effect was much more pronounced at high values of  $L$ , being negligible at  $L = 1.2$  and a factor of ten at  $L = 1.8$ . Moreover the effect was greater for a given  $L$  at larger values of  $B/B_0$  (i.e., for lower mirror points). Both of these effects are in qualitative agreement with the basic geometry of particle injection by neutron albedo originating in the polar caps. It is fortunate that there were also good satellite observations of the absolute solar cosmic ray intensity during the event as well as its latitude dependence (Lin, 1961). Work is now in progress to find whether or not quantitative agreement exists.

#### 4.2 SOURCES OF TRAPPED PARTICLES AND/OR KINETIC ENERGY IN THE OUTER ZONE

The outer zone is characterized by an almost complete absence of high-energy protons. An upper limit of  $1 \times 10^2/\text{cm}^2 \text{ sec}$  of protons of energy greater than 60 Mev was placed by Pioneer IV (Van Allen and Frank, 1959). The more recent Explorer VI measurements with a lead-shielded coincidence telescope by Fan, Meyer, and Simpson (1960) has driven the upper limit of the intensity of protons of  $E > 75$  Mev down to  $0.1/\text{cm}^2 \text{ sec}$ . There is no information of significance on the intensities of protons of energy less than 30 Mev.

The outer boundary of the outer zone has been observed by means of substantially the same instrument (a single Geiger tube shielded by about  $1 \text{ g/cm}^2$ ) to fluctuate over the radial range 95 000 km (15 Earth radii) to about 40 000 km (6.3 Earth radii) in the equatorial plane. There is usually a major peak of intensity at a radial distance of about 22 000 km (3.5 Earth radii), though the position of the peak varies somewhat, and during some periods of time the peak has been observed to be bifurcated into two or more comparable peaks. Among the various measurements over the past three years, the magnitude of the intensity in the vicinity of 3.5 Earth radii has been observed to vary by nearly two orders of magnitude. Generally speaking the fluctuations are closely associated with solar and geomagnetic activity, though the association is not of a simple nature. (See Forbush, Venkatesan, and McIlwain, 1961). The following general pattern has begun to emerge, though it should not be regarded as universal:

F

(a) Within a time of the order of a few hours to a day after the onset of a geomagnetic storm, the content of the outer zone (as measured with a thinly shielded Geiger tube which has an electron-bremsstrahlung threshold of about 20 keV) is markedly depleted. The depletion may be by as much as an order of magnitude or more. On several occasions of large events there have been notable sub-auroral zone aurorae and red arcs lying along a locus of  $L \sim 3.5$  Earth radii (O'Brien, Van Allen, Roach and Gartlein, 1960), (O'Brien and Ludwig, 1960), (Arnoldy, Hoffman and Winckler, 1960). Also during this 'dumping' phase the ring current parameter of Kertz *increases*, apparently signifying an *increase* in the quantity of low energy protons and electrons (not directly observed with techniques used thus far) in trapped or quasi-trapped orbits after the manner of Chapman and Ferraro and of Alfvén.

(b) Then with a time constant again of the order of one day the observable intensity of electrons undergoes a strong increase and reaches a level equal to or perhaps an order of magnitude greater than its pre-storm value. During this period the ring current declines toward its quiescent value.

(c) Finally the intensity of observable electrons in the outer zone relaxes back toward its quiescent level with a time constant of the order of a week or more.

One of the best observed and most interesting case histories of an occasion such as described above occurred during early April 1960. During this period Explorer VII was making a regular patrol of the outer zone at an altitude of  $\sim 1000$  kilometers and Pioneer V was measuring the particle intensity and the interplanetary magnetic field at a distance of  $\sim 0.03$  A.U., (i.e., at a position well outside of the geomagnetic field but in the near-astronomical vicinity of the Earth.) (Van Allen and Lin, 1960), (Arnoldy, Hoffman and Winckler, 1960), (Coleman, Sonett, Judge and Smith, 1960).

Figure 4.1 shows on a common time scale the peak counting rate of the thinly shielded counter in the outer zone (Explorer VII), the magnetic measurements in Pioneer V, and the ground station record of the geomagnetic field intensity at Iowa City. Also of essential significance are the simultaneous observations of Winckler *et al* (also in Pioneer V) of the particle intensity measured with a Geiger tube nearly identical with the one in Explorer VII; in sharp contrast with the Geiger tube rates shown in Figure 4.1 Winckler observed an increase above cosmic ray rate of at most one count per second during the magnetic peak of Coleman *et al*.

The following interpretation of this combination of observations is proposed.

(a) The magnetometer in Pioneer V recorded the passage of a major burst of ionized, magnetized solar plasma.

(b) This plasma contained a negligible intensity of electrons with energies exceeding 20 keV.

(c) The arrival of the plasma at the Earth (with trivial time-lag on the scale shown) produced a major magnetic storm, perturbed the orbits of previously existing trapped electrons of energies in the range of tens of kilo-electron volts thus causing the dumping of a large fraction of the energy of the outer zone into the atmosphere to produce the widespread, brilliant, low-latitude aurora which was observed during this period.

(d) During this process a portion of the low-energy plasma was entrapped by the geomagnetic field.

(e) The low-energy particles which thus became a part of the outer zone were subsequently accelerated to a level of observability by magnetic and hydromagnetic processes of unknown detailed character.

(f) Finally by virtue of energy loss and other perturbations of more usual character and magnitude the outer zone intensity relaxed back to the quiescent level which is presumably maintained by a quiescent solar wind.

On the basis of this type of evidence, the present author feels that there is overwhelming evidence that the outer zone owes its existence to solar plasma and to local accelerating processes of a magnetic nature in the Earth's field. Whether or not the particles being detected are the very same ones which arrived in the solar plasma or whether they are ones belonging

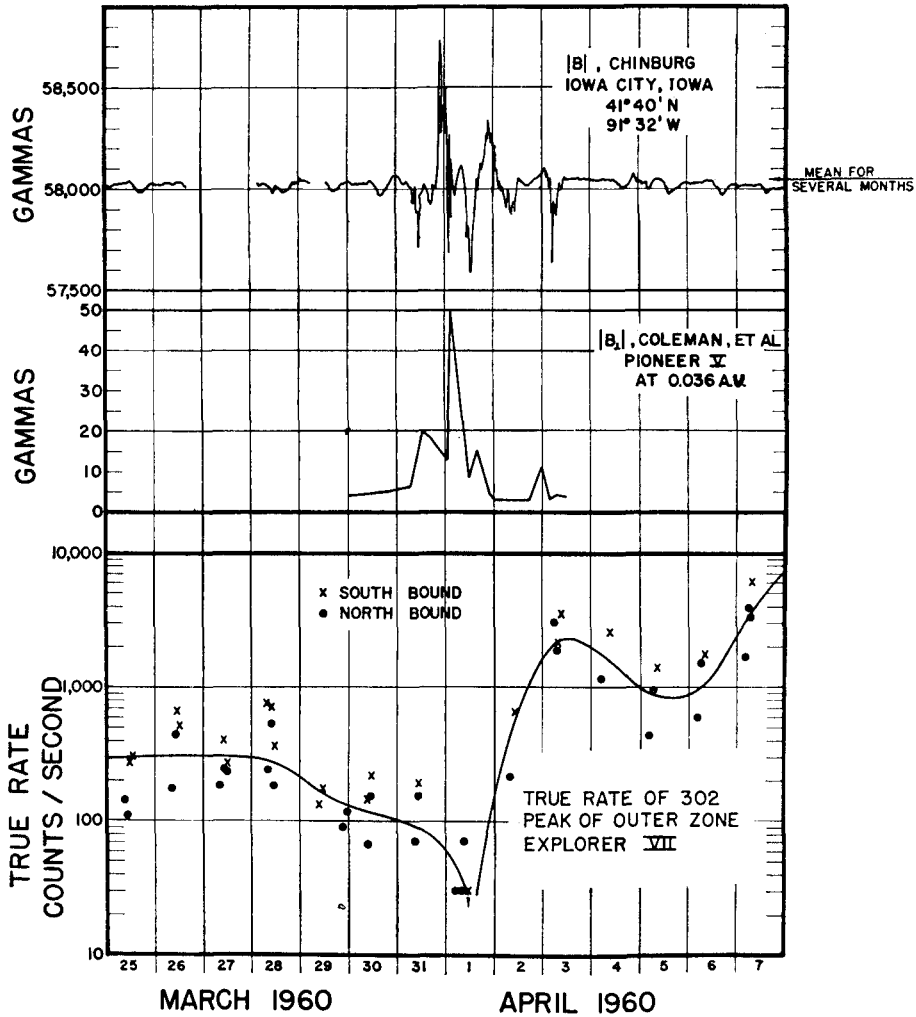


Fig. 4.1. The time relationship of (a) the maximum intensity in the low altitude portion of the outer zone (b) the interplanetary magnetic field at 0.03 A.U. and the ground station record of  $B$  (after Van Allen).

to the Earth's system prior to the arrival of the solar plasma is irrelevant. The essential aspect of the belief is that the energy for producing and maintaining the outer zone is from the Sun. Furthermore there is no significant suggestion that the necessary energy can be delivered to the outer zone in any other form than as kinetic energy of solar plasma.

There remains a wide variety of fascinating problems associated with the origin and dynamics of the outer zone and with the relationship of the outer zone to aurorae, airglow, geomagnetic

activity and atmospheric heating. No attempt to treat these problems has been made in the present paper.

Moreover even direct observational knowledge of the absolute intensities and energy spectra of electrons and protons in the outer zone is in a quite preliminary state. On the basis of the single assumption that the intensity of electrons of energies exceeding 2.2 Mev does not exceed  $10^{-6}$  of those of lesser energy, the author has given the experimentally-based estimate of  $10^{11}$  (cm<sup>2</sup> sec)<sup>-1</sup> as the omni-directional intensity of electrons of energy exceeding 40 keV in the heart of the outer zone on 3 March 1959 (a date of exceptionally high intensity); and in spite of considerable later evidence some of a confirmatory and some of a conflicting nature (See for example collection of papers in *Space Research*, edited by H. K. Kallman-Bijl, 1960), he still finds it very difficult to accept a figure less than about  $10^{10}$  (cm<sup>2</sup>sec)<sup>-1</sup> as typifying the intensity of electrons in the tens to hundreds of kilo-electronvolt energy range in the heart of the outer zone.

There remains a pressing need for more decisive experiments in the area. Such experiments are currently under way.

#### 4.3 REFERENCES

- Alfvén, H. *Cosmical Electrodynamics* Oxford, Clarendon Press, 237 pp., 1950.
- Armstrong, A. H., Harrison, F. B. and Rosen, L. Flux and Energy of Charged Particles at 300- and 600-mile Altitude *Bull. Amer. Phys. Soc.* **4**, 360, 1959.
- Armstrong, A. H., Harrison, F. B., Heckman, H. H. and Rosen, L. Charged Particles in the Inner Van Allen Radiation Belt *J. geophys. Res.* **66**, 351-357, 1961.
- Arnoldy, R. L., Hoffman, R. A. and Winckler, J. R. Observations of the Van Allen Radiation Regions during August and September 1959, Part I *J. geophys. Res.* **65**, 1361-1375, 1960.
- Bennett, W. H. Solar Proton Stream Forms with a Laboratory Model *Rev. Sci. Instr.* **30**, 63-69, 1959.
- Birkeland, Kr. *The Norwegian Aurora Polaris Expedition, Volume I On the Cause of Magnetic Storms and the Origin of Terrestrial Magnetism. First Section pp. 1-315, Plates I-XXI, 1908. Second Section pp. 319-801, Plates XXII-XLII, 1913.* Christiania, Norway, H. Aschehong and Co. (English).
- Block, L. Model Experiments on Aurorae and Magnetic Storms *Tellus*, **7**, 65-86, 1955.
- Brüche, E. Some New Theoretical and Experimental Results on the Aurora Polaris *Terr. Mag. and atmos. Electricity*, **36**, 41-52, 1931.
- Chapman, S. and Bartels, J. *Geomagnetism*, Vols. I and II Oxford, Clarendon Press, 1049 pp., 1940.
- Christofilos, N. C. Various classified memoranda, U. S. Atomic Energy Commission, 1958.
- Christofilos, N. C. The Argus Experiment *J. geophys. Res.* **64**, 869-875, 1959.
- Coleman, P. J., Jr., Sonett, C. P. and Judge, D. L. Some Preliminary Results of the Pioneer V Magnetometer Experiment *J. geophys. Res.* **65**, 1856-1857, 1960.
- Dragt, A. J. Effect of Hydromagnetic Waves on the Lifetime of Van Allen Radiation Protons *J. geophys. Res.* **66**, 1641-1649, 1961.
- Dresden M. Private Communication, 1961.
- Fan, C. Y., Meyer, P. and Simpson, J. A. Trapped and Cosmic Radiation Measurements from Explorer VI pp. 951-966 of *Space Research* (Proceedings of the First International Space Science Symposium), ed. H. K. Kallman-Bijl, Amsterdam, North Holland Publishing Co., 1195 pp., 1960.
- Forbush, S. E., Venkatesan, D. and McIlwain, C. E. Intensity Variations in Outer Van Allen Radiation Belt *J. geophys. Res.* **66**, 2275-2287, 1961.

- Freden, S. C. and White, R. S. Protons in the Earth's Magnetic Field *Phys. Rev. Letters* **3**, 9-10, 1959 and **3**, 145, 1959.
- Freden, S. C. and White, R. S. Particle Fluxes in the Inner Radiation Belt *J. geophys. Res.* **65**, 1377-1383, 1960.
- Ganges, A. V., Jenkins, J. F., Jr. and Van Allen, J. A. The Cosmic-Ray Intensity Above the Atmosphere *Phys. Rev.* **75**, 57-69, 1949.
- Gibson, G., Jordan, W. C. and Lauer, E. J. Containment of Positrons in a Mirror Machine *Phys. Rev. Letters* **5**, 141-144, 1960.
- Hamlin, D. A., Karplus, R., Vik, R. C. and Watson, K. M. Mirror and Azimuthal Drift Frequencies for Geomagnetically Trapped Particles *J. geophys. Res.* **66**, 1-4, 1961.
- Hess, W. N. Van Allen Belt Protons from Cosmic-Ray Neutron Leakage *Phys. Rev. Letters*, **3**, 11-13, 1959, and **3**, 145, 1959.
- Hess, W. N., Patterson, H. W., Wallace, R. and Chupp, E. L. Cosmic-Ray Neutron Energy Spectrum *Phys. Rev.* **116**, 445-457, 1959.
- Hess, W. N. and Starnes, A. J. Measurement of the Neutron Flux in Space *Phys. Rev. Letters*, **5**, 48-50, 1960.
- Hess, W. N., Canfield, E. H. and Lingenfelter, R. E. Cosmic-Ray Neutron Demography *J. geophys. Res.* **66**, 665-677, 1961.
- Holly, F. E. and Johnson, R. G. Measurement of Radiation in the Lower Van Allen Belt *J. geophys. Res.* **65**, 771-772, 1960.
- Holly, F. E., Allen, L., Jr. and Johnson, R. G. Radiation Measurements to 1500 Kilometers Altitude at Equatorial Latitudes *J. geophys. Res.* **66**, 1627-1639, 1961.
- Jensen, D. C., Murray, R. W. and Welch, J. A. Jr. Tables of Adiabatic Invariants for the Geomagnetic Field 1955.0 AFSWC-TN-60-8, 109 pp, April 1960. AFSWC-TN-60-19, 77 pp, August 1960. (unpublished) Air Force Special Weapons Center Kirtland Air Force Base, New Mexico.
- Kallman-Bijl, H. K. *Space Research* (Proceedings of the First International Space Science Symposium), North Holland Publishing Co., Amsterdam, 1195 pp, 1960.
- Kasper, J. E. Geomagnetic Effects on Cosmic Radiation for Observation Points Above the Earth *J. geophys. Res.* **65**, 39-53, 1960.
- Kellogg, P. J. Possible Explanation of the Radiation Observed by Van Allen at High Altitudes in Satellites *Nuovo Cim. Serie X*, **11**, 48-66, Gennaio, 1959.
- Kellogg, P. J. Electrons of the Van Allen Radiation *J. geophys. Res.* **65**, 2705-2713, 1960.
- Kertz, W. Ein Neues Mass für die Feldstärke des Erdmagnetischen Äquatorialen Ringstrom *Abhandlungen, Akad. Wiss. Göttingen Mathematisch-Physikalische Klasse Beiträge zum Internationalen Geophysikalischen Jahr, Heft 2*. Göttingen, Vandenhoeck and Ruprecht, 1958.
- Krassovsky, V. I., Shklovsky, I. S., Galperin, G. I. and Svetlitsky, E. M. On Fast Corpuscles of the Upper Atmosphere pp. 59-63 of *Proceedings of the Moscow Cosmic Ray Conference*, Vol. III, ed. S. I. Syrovatsky, Int. U. Pure Applied Phys., Moscow, 1960.
- Kulenkampf, H. Bemerkung zum Intensitätsverlauf der Ultrastrahlung in grössen Höhen *Die Naturwissenschaften*, **21**, 25-26, 1933.
- Lew, J. S. Drift Rate in a Dipole Field *J. geophys. Res.* **66**, 2681-2685, 1961.
- Lin, W. C. and Van Allen, J. A. Private Communication, 1960.
- Lin, W. C. Observation of Galactic and Solar Cosmic Rays from October 13, 1959 to February 17, 1961 with Explorer VII (Satellite 1959 Iota) State University of Iowa Research Report 61-16, August 1961. (unpublished).
- Malmfors, K. G. Determination of Orbits in the Field of a Magnetic Dipole with Applications to the Theory of the Diurnal Variation of Cosmic Radiation *Arkiv för Matem., Astr. och Fys.* **32A**, No. 8, 64 pp. 1945.
- Martyn, D. F. The Theory of Magnetic Storms and Auroras *Nature, Lond.* **167**, 92-94, 1951.
- McIlwain, C. E. Private Communication, 1960.
- McIlwain, C. E. and Rothwell, P. Spatial Dependence of the Intensity of Charged Particles Trapped in the Earth's Field Between 50°N and 50°S Geographic Latitude, and 300- to 2000-km. Altitude *J. geophys. Res.* **65**, 2508-2509, 1960 (Abstract).

- McIlwain, C. E. Coordinates for Mapping the Distribution of Magnetically Trapped Particles *J. geophys. Res.* **66**, 3681–3691, 1961.
- Naugle, J. E. and Kniffen, D. A. Flux and Energy Spectrum of the Protons in the Inner Van Allen Belt *Phys. Rev. Letters* **7**, 3–6, 1961.
- Northrup, T. G. and Teller, E. Stability of the Adiabatic Motion of Charged Particles in the Earth's Field *Phys. Rev.* **117**, 215–225, 1960.
- O'Brien, B. J. and Ludwig, G. H. Development of Multiple Radiation Zones on October 18, 1959 *J. geophys. Res.* **65**, 2696–2699, 1960.
- O'Brien, B. J., Van Allen, J. A., Roach, F. E. and Gartlein, C. W. Correlation of an Auroral Arc and a Subvisible Monochromatic 6300Å. Arc with Outer-Zone Radiation on 28 November 1959 *J. geophys. Res.* **65**, 2759–2766, 1960.
- Parker, E. N. Effect of Hydromagnetic Waves in a Dipole Field on the Longitudinal Invariant *J. geophys. Res.* **66**, 693–708, 1961.
- Pennington, R. H. Equation of a Charged Particle Shell in a Perturbed Dipole Field *J. geophys. Res.* **66**, 709–712, 1961.
- Pizzella, G. Private Communication, 1961.
- Poincaré, H. Remarques sur une expérience de M. Birkeland *C. R. Acad. Sci., Paris* **123**, 930, 1896.
- Ray, E. C. On the Application of Liouville's Theorem to the Intensity of Radiation Trapped in the Geomagnetic Field. State University of Iowa Research Report 59–21, 1959 (unpublished).
- Ray, E. C. Private Communication, 1960.
- Ray, E. C. On the Theory of Protons Trapped in the Earth's Magnetic Field *J. geophys. Res.* **65**, 1125–1134, 1960.
- Rodionov, S. N. An Experimental Test of the Behaviour of Charged Particles in an Adiabatic Trap *J. Nuclear Energy, Part C, Plasma Physics* **1**, 247–252, 1960.
- Rosen, A., Farley, T. A. and Sonett, C. P. Soft Radiation Measurements on Explorer VI Earth Satellite pp. 938–950 of *Space Research* (Proceedings of the First International Space Science Symposium), ed. H. K. Kallman-Bijl, Amsterdam, North Holland Publishing Co., 1195 pp., 1960.
- Rossi, B. Interpretation of Cosmic-Ray Phenomena *Rev. Mod. Phys.* **20**, 537–583, 1948.
- Rothwell, P. and McIlwain, C. E. Magnetic Storms and the Van Allen Radiation Belts: Observation with Satellite 1958ε (Explorer IV) *J. geophys. Res.* **65**, 799–806, 1960.
- Singer, S. F. A New Model of Magnetic Storms and Aurorae *Trans. Am. Geophys.* **38**, 175–190, 1957.
- Singer, S. F. Radiation Belt and Trapped Cosmic Ray Albedo *Phys. Rev. Letters* **1**, 171–173, 1958.
- Singer, S. F. Trapped Albedo Theory of the Radiation Belt *Phys. Rev. Letters* **1**, 181–183, 1958.
- Singer, S. F. Cause of the Minimum in the Earth's Radiation Belt *Phys. Rev. Letters* **3**, 188–190, 1959.
- Singer, S. F. Latitude and Altitude Distribution of Geomagnetically Trapped Protons *Phys. Rev. Letters* **5**, 300–303, 1960.
- Singer, S. F. On the Nature and Origin of the Earth's Radiation Belts pp. 797–820 of *Space Research* (Proceedings of the First International Space Science Symposium), ed. H. K. Kallman-Bijl, Amsterdam, North Holland Publishing Co., 1195 pp., 1960.
- Spitzer, L., Jr. *Physics of Fully Ionized Gases* New York, Interscience Publishers, Inc., 105 pp. 1956.
- Störmer, C. Sur les trajectoires des corpuscles électrisés dans l'espace sous l'action du magnétisme terrestre Chapitre IV, *Arch. Sci. phys. et naturelles* **24**, 317–364, 1907.
- Störmer, C. *The Polar Aurora* Oxford, Clarendon Press, 403 pp. and 213 figures, 1955.
- Vallarta, M. S. *An Outline of the Theory of the Allowed Cone of Cosmic Radiation* University of Toronto Studies, Applied Mathematics Series No. 3, University of Toronto Press, 56 pp., 1938.
- Van Allen, J. A. and Tatel, H. E. The Cosmic-Ray Counting Rate of a Single Geiger Counter from Ground Level to 161 Kilometers Altitude *Phys. Rev.* **73**, 245–251, 1948.

- Van Allen, J. A. and Singer, S. F. On the Primary Cosmic-Ray Spectrum *Phys. Rev.* **78**, 819 and **80**, 116, 1950.
- Van Allen, J. A. Direct Detection of Auroral Radiation with Rocket Equipment *Proc. Nat. Acad. Sci.* **43**, 57-92, 1957.
- Van Allen, J. A. Special joint meeting of National Academy of Sciences and American Physical Society, Washington, D.C., 1 May 1958. IGY Satellite Report Number 13, January 1961, IGY World Data Center A, Rockets and Satellites—National Academy of Sciences, National Research Council, Washington 25, D.C.
- Van Allen, J. A., Ludwig, G. H., Ray, E. C. and McIlwain, C. E. Observation of High Intensity Radiation by Satellites 1958 Alpha and Gamma *Jet Propulsion* **28**, 588-592, 1958.
- Van Allen, J. A. and Frank, L. A. Radiation Around the Earth to a Radial Distance of 107,400 Kilometers *Nature, Lond.* **183**, 430-434, 1959.
- Van Allen, J. A., McIlwain, C. E. and Ludwig, G. H. Radiation Observations with Satellite 1958e *J. geophys. Res.* **64**, 271-286, 1959.
- Van Allen, J. A., McIlwain, C. E. and Ludwig, G. H. Satellite Observations of Electrons Artificially Injected into the Geomagnetic Field *J. geophys. Res.* **64**, 877-891, 1959.
- Van Allen, J. A. and Frank, L. A. Radiation Measurements to 658,300 Km. with Pioneer IV *Nature, Lond.* **184**, 219-224, 1959.
- Van Allen, J. A. The Geomagnetically-Trapped Corpuscular Radiation *J. geophys. Res.* **64**, 1683-1689, 1959.
- Van Allen, J. A. and Lin, W. C. Outer Radiation Belt and Solar Proton Observations with Explorer VII during March-April 1960 *J. geophys. Res.* **65**, 2998-3003, 1960.
- Vernov, S. N., Grigorov, N. I., Logachev, Yu. I. and Chudakov, A. Ye. Artificial Satellite Measurements of Cosmic Radiation, *Dokl. Akad. Nauk S.S.S.R.* **120**, 1231-1233, 1958.
- Vernov, S. N. (and Lebedinsky, A. I.) Special Lecture, Fifth General Assembly of CSAGI in Moscow, July 30—August 9, 1958. Also New York Times, Friday, 1 August, 1958.
- Vernov, S. N., Chudakov, A. E., Vakulov, P. V. and Logachev, Yu. I. Study of Terrestrial Corpuscular Radiation and Cosmic Rays by the Flight of a Cosmic Rocket *Dokl. Akad. Nauk S.S.S.R.* **125**, 304-307, 1959.
- Vernov, S. N., Chudakov, A. E., Gouchakov, E. V., Logachev, J. L. and Vakulov, P. V. Study of the Cosmic-Ray Soft Component by the 3rd Soviet Earth Satellite *Plan. Space Sci.* **1**, 86-93, 1959.
- Vernov, S. N. and Chudakov, A. E. Investigation of Radiation in Outer Space. pp. 19-29 of *Proceedings of the Moscow Cosmic Ray Conference*, Vol. III, ed. S. I. Syrovatsky, Int. U. Pure Applied Phys. Moscow, 1960.
- Vernov, S. N. and Chudakov, A. E. Terrestrial Corpuscular Radiation and Cosmic Rays. pp. 751-796 of *Space Research* (Proceedings of the First International Space Science Symposium), ed. H. K. Kallman-Bijl, Amsterdam, North Holland Publishing Co., 1195 pp., 1960.
- Vernov, S. N., Chudakov, A. E., Vakulov, P. V., Logachev, Yu. I. and Nikolaev, A. G. Radiation Measurements During the Flight of the Second Cosmic Rocket, *Dokl. Akad. Nauk S.S.S.R.* **130**, 517-520, 1960.
- Vestine, E. H. Note on Conjugate Points of Geomagnetic Field Lines for Some Selected Auroral and Whistler Stations of the I.G.Y. *J. geophys. Res.* **64**, 1411-1414, 1959.
- Vestine, E. H. and Sibley, W. L. The Geomagnetic Field in Space, Ring Currents, and Auroral Isochasms *J. geophys. Res.* **65**, 1967-1979, 1960.
- Vestine, E. H. and Sibley, W. L. *Geomagnetic Field Lines in Space*, Project Rand Report No. R-368, December 1960, The Rand Corporation, Santa Monica, California, 111 pp., 1961.
- Walt, M., Chase, L. F., Jr., Cladis, J. B., Imhof, W. L. and Knecht, D. J. Energy Spectra and Altitude Dependence of Electrons Trapped in the Earth's Magnetic Field pp. 910-920 of *Space Research* (Proceedings of the First International Space Science Symposium), ed. H. K. Kallman-Bijl, Amsterdam, North Holland Publishing Co., 1195 pp., 1960.
- Welch, J. A., Jr. and Whitaker, W. A. Theory of Geomagnetically Trapped Electrons from an Artificial Source *J. geophys. Res.* **64**, 909-922, 1959.
- Wentzel, D. G. Hydromagnetic Waves and the Trapped Radiation, Part 1. Breakdown of the Adiabatic Invariance. Part 2. Displacements of the Mirror Points *J. geophys. Res.* **66**, 359-362 and 363-369, 1961.

- Yagoda, H. Star Production by Trapped Protons in the Inner Radiation Belt *Phys. Rev. Letters*, **5**, 17–18, 1960.
- Yoshida, S., Ludwig, G. H. and Van Allen, J. A. Distribution of Trapped Radiation in the Geomagnetic Field *J. geophys. Res.* **65**, 807–813, 1960.